

Alternative Conditioning Method to Calculate Formation Factor for Wisconsin Concrete Pavement

Jussara Tanesi, Ph.D., FAcI

American Engineering Testing

WisDOT ID no. 0092-24-04

August 2025



RESEARCH & LIBRARY UNIT



WISCONSIN HIGHWAY RESEARCH PROGRAM

WISCONSIN DOT
PUTTING RESEARCH TO WORK

1. Report No. 0092-24-04		2. Government Accession No.		3. Recipient's Catalog No.	
4. Title and Subtitle Alternative Conditioning Method to Calculate Formation Factor for Wisconsin Concrete Pavement				5. Report Date August, 2025	
				6. Performing Organization Code	
7. Author(s) Jussara Tanesi, Ph.D., FACI				8. Performing Organization Report No. If applicable, enter any/all unique numbers assigned to the performing organization.	
9. Performing Organization Name and Address American Engineering Testing - AET				10. Work Unit No.	
				11. Contract or Grant No. WHRP 0092-24-04	
12. Sponsoring Agency Name and Address Wisconsin Department of Transportation Research & Library Unit 4822 Madison Yards Way Room 911 Madison, WI 53705				13. Type of Report and Period Covered Final Report October 2023 - September 2025	
				14. Sponsoring Agency Code	
15. Supplementary Notes N/A					
16. Abstract Formation factor has been identified as one of the main properties related to concrete transport properties. Conditioning specimens in solution, such as the default conditioning in ASTM C1876 has been proposed as a means to obtain the formation factor. However, this conditioning has been criticized for several reasons. This project investigates the effect of different conditionings on bulk resistivity and formation factor. A total of 19 mixtures were evaluated, and six conditioning methods were investigated. Estimation of the pore solution resistivity was also investigated. It was observed that conditioning affected the degree of reaction and the pore structure, and as a result, bulk resistivity and formation factor. The modified NIST model (Montanari model) was revised and provided good estimation of the pore solution resistivity that can be used to determine the formation factor. For mixture qualification purposes, it was recommended to use sealed specimens and to estimate the pore solution resistivity through modeling and then determine the formation factor. For QA/QC purposes, it was recommended to determine the bulk resistivity of specimens cured in limewater or specimens subjected to accelerated curing.					
17. Key Words Electrical resistivity, formation factor, concrete, surface resistivity, bulk resistivity, conditioning, service life, porosity, transport properties			18. Distribution Statement No restrictions. This document is available through the National Technical Information Service. 5285 Port Royal Road Springfield, VA 22161		
19. Security Classif. (of this report) Unclassified		20. Security Classif. (of this page) Unclassified		21. No. of Pages 49	22. Price

DISCLAIMER

This research was funded through the Wisconsin Highway Research Program by the Wisconsin Department of Transportation and the Federal Highway Administration under Project 0092-24-04. The contents of this report reflect the views of the authors who are responsible for the facts and accuracy of the data presented herein. The contents do not necessarily reflect the official views of the Wisconsin Department of Transportation or the Federal Highway Administration at the time of publication.

This document is disseminated under the sponsorship of the Department of Transportation in the interest of information exchange. The United States Government assumes no liability for its contents or use thereof. This report does not constitute a standard, specification or regulation.

The United States Government does not endorse products or manufacturers. Trade and manufacturers' names appear in this report only because they are considered essential to the object of the document.

Table of Contents

1. Executive Summary	1
2. Introduction.....	2
3. Research need statement.....	3
4. Research Objectives.....	3
5. Literature Review.....	3
5.1.1.1. Concrete Electrical resistivity.....	3
5.1.1.2. Formation Factor.....	5
6. Research Plan.....	9
6.1. Materials	9
6.2. Phase I – Effect of Conditioning on the Electrical Resistivity and Formation Factor....	9
6.2.1. Mixture Selection.....	10
6.2.2. Phase I - Mixture Preparation and Conditioning	11
6.2.3. Phase I - Testing.....	11
6.3. Phase 2 – Mixtures’ Preparation and Testing	15
6.3.1. Phase II - Mixture Preparation and Conditioning	16
6.3.2. Effect of Coarse Aggregate.....	17
6.3.3. Effect of w/cm.....	17
6.3.4. Effect of Cement Replacement	18
6.3.5. Effect of Cement	19
6.3.6. Effect of Conditioning	19
7. Results.....	21
7.1. Materials’ Testing	21
7.2. Phase 1 Testing	22
7.2.1. Bulk Resistivity.....	22
7.2.2. Pore Solution Resistivity obtained through Modeling.....	24
7.2.3. Pore Solution Electrical Resistivity Obtained Experimentally.....	25
7.2.4. Porosity	26
7.2.5. Formation Factor.....	27
7.2.6. Service Life.....	28
7.3. Phase 2 Testing	32

7.3.1.	Effect of Conditioning	32
7.3.2.	Effect of the Coarse Aggregate	34
7.3.3.	Effect of the w/cm.....	36
7.3.4.	Effect of the % of Cement Replacement.....	37
7.3.5.	Effect of Cement	39
7.3.6.	Effect of Age.....	41
7.3.7.	Relationship between Surface Resistivity and Bulk resistivity	41
7.3.8.	Relationship between Bulk Resistivity and RCPT	42
8.	Conclusions and Recommendations	43
8.1.	Recommendations.....	43
8.1.1.	Recommended Specification Language.....	45
9.	References.....	45
	Appendix A	

List of Figures

Figure 1 – Relationship between surface resistivity and RCPT in three studies[10].	4
Figure 2 – Factors affecting concrete resistivity; (a) Porosity and solids; (b) saturation, (c) ionic concentration of the pore solution, (d) pores connectivity. (Adapted from Spragg <i>et al.</i> [15] and Tanesi <i>et al.</i> [16]).	4
Figure 3 – (a) Poorer concrete microstructure leads to lower concrete resistivity (concrete A), (b) concrete higher degree of saturation and higher ionic concentration of the pore solution lead to lower resistivity (concrete B), (c) combination of microstructure and pore solution result in the same resistivity for concretes A and B [1].	5
Figure 4 – (a) Schematics of the pore solution expression apparatus; (b) Resistivity cell for pore solution measurements [21].	6
Figure 5 – Pore solution resistivity (a) OPC mixtures, (b) Binary mixtures with fly ashes, and (c) Binary mixtures with slag cement. Values in y-axis were calculated based on the ionic concentrations of species.	7
Figure 6 – Schematic of the concentrated alkali conditioning solution procedure on a concrete cylinder specimen. Red-dash dots are gel pores saturated with the mixture’s original pore solution (at the time of specimen immersion); half-red-dash dots are matrix pores partially filled with the original pore solution; red-blue dash dots are matrix pores filled with the alkali-concentrated conditioning solution and partially filled with the original pore solution; blue dots indicate pores filled with the alkali-concentrated conditioning solution; and big white dots represent non-filled entrained air voids.	9
Figure 7 – Project plan for Phase I.	10
Figure 8 – Variables for the determination of the pore solution resistivity.	10
Figure 9 – Determination of the pore solution resistivity.	12
Figure 10 – Pore solution resistivity. (a) resistivity cell, (b) resistivity set up, (c) dimensions of the stainless-steel plates of the resistivity cells, and (d) dimensions of the polycarbonate tube of the resistivity cell.	14
Figure 11 – Influence of aggregates testing matrix. BR stands for bulk resistivity (ASTM C1876), SR stands for surface resistivity (WTM T358), RCPT stands for rapid chloride penetrability test (ASTM C1202), and PS stands for pore solution.	17
Figure 12 – Influence of w/cm testing matrix. BR stands for bulk resistivity (ASTM C1876), SR stands for surface resistivity (WTM T358), and RCPT stands for rapid chloride penetrability test (ASTM C1202).	18
Figure 13 – Influence of cement replacement testing matrix. BR stands for bulk resistivity (ASTM C1876), SR stands for surface resistivity (WTM T358), RCPT stands for rapid chloride penetrability test (ASTM C1202), and PS stands for pore solution.	19

Figure 14 – Influence of cement testing matrix. BR stands for bulk resistivity (ASTM C1876), and RCPT stands for rapid chloride penetrability test (ASTM C1202).	19
Figure 15 – Influence of SCM testing matrix. BR stands for bulk resistivity (ASTM C1876), SR stands for surface resistivity (WTM T358), RCPT stands for rapid chloride penetrability test (ASTM C1202), and PS stands for pore solution.	20
Figure 16 –Bulk resistivity over time for (a) Coal creek mixture, (b) Elm Road mixture, (c) Slag mixture, and (d) Reclaimed Ash mixture. LW stands for limewater, DC for default conditioning (pore solution), and SL for sealed. Error bars indicate ± 1 standard deviation.	23
Figure 17 – Pore solution resistivity obtained using the resistivity cell, by determining the chemical composition by ion chromatography (IC) and then calculating the pore solution resistivity (Snyder <i>et al.</i> [23]) or estimated by the revised Montanari model. Pore solution resistivity was determined at 91 days for limewater and default conditioning, and at 56 days for sealed condition.....	25
Figure 18 – Formation factor calculated using different means of obtaining pore solution resistivity. Cell indicates formation factor calculated using pore solution resistivity obtained using the pore solution cell, IC indicates that chemical composition was determined by ion chromatography and formation factor was calculated using pore solution resistivity obtained by the Snyder <i>et al.</i> [23] model, and Def, formation factor was calculated using the default value for the pore solution resistivity.....	27
Figure 19 – Bulk resistivity of sealed specimens at 56 days. Bulk resistivity of AC at 28 days and all other conditionings at 91 days.	33
Figure 20 – Effect of conditioning on formation factor. Horizontal lines indicate requirements in AASHTO R 101. FF of AC at 28 days and all other conditionings at 91 days.	34
Figure 21 – Effect of coarse aggregate on bulk resistivity at 91 days.	35
Figure 22 – Effect of coarse aggregate on formation factor at 91 days. Horizontal lines indicate requirements in AASHTO R 101.....	35
Figure 23 – Effect of w/cm on bulk resistivity.	36
Figure 24 – Effect of w/cm on formation factor at 91 days. Horizontal lines indicate requirements in AASHTO R 101.....	37
Figure 25 – Effect of % cement replacement on bulk resistivity.....	38
Figure 26 – Effect of % cement replacement on formation factor. AC at 28 days and DC at 91 days. Horizontal lines indicate requirements in AASHTO R 101.	39
Figure 27 – Effect of cement on bulk resistivity. Sealed at 56 days, other conditionings at 91 days.	40
Figure 28 – Effect of cement on formation factor with default conditioning. Horizontal lines indicate requirements in AASHTO R 101.	40
Figure 29 – Effect of age on bulk resistivity.....	41

Figure 30 – Correlation between surface resistivity and bulk resistivity. (a) by conditioning type, (b) all data. Dashed line indicates $\pm 10\%$ 41

Figure 31 – Correlation between bulk resistivity and RCPT. Circled points indicate mismatch in classification between resistivity and RCPT..... 42

Figure 32 – Recommendation for implementation of formation factor for mixture qualification and resistivity for QA/QC..... 44

1. EXECUTIVE SUMMARY

Formation factor has been identified as one of the main properties related to concrete transport properties. Conditioning specimens in solution, such as the default conditioning in ASTM C1876 has been proposed as a means to obtain the formation factor. However, this conditioning has been criticized as it requires large solution amounts of the solution, which is typically regulated as hazardous waste and requires proper handling and disposal. Moreover, the equilibrium between the pore solution and the conditioning solution is not always achieved, even after 90 days of conditioning, resulting in inaccurate formation factors.

In this study, an extensive experimental program was carried out where the effect of different concrete conditionings on bulk resistivity, formation factor, microstructure and service life was evaluated. The effect of materials and mixture proportions on bulk resistivity and formation factor was also assessed.

It was found that the conditioning method may affect the reaction kinetics and the pore structure. This subsequently affects the bulk resistivity and the formation factor, and, as a result, impacts the predicted service life of the concrete.

Based on the results of this study, the most practical means for determining formation factor was found to be using sealed specimens in the mixture qualification stage. Then, the bulk resistivity of specimens cured in limewater can be used for quality control purposes.

2. INTRODUCTION

The Federal Highway Administration has been promoting a shift from a prescriptive to a performance-based approach to concrete-mixture design for pavement applications. Among the selected performance requirements, transport properties, how easily fluids and ions move through the hardened concrete, occupy an important role as they are directly related to the durability of concrete. The related interest in being able to quickly assess the transport properties of concrete mixtures has brought the community to focus on electrically-based tests [1], [2], [3], [4]. There has been a growing interest in implementing concrete electrical resistivity and formation factor (FF) as performance requirements in State DOTs specifications. Requirements based on electrical resistivity have been incorporated in several specifications and applied as a quality control/assurance method both in the United States and abroad [5], [6], [7].

However, there are several concerns regarding implementing either concrete electrical resistivity or FF on the specifications. Concrete electrical resistivity is affected not only by the concrete microstructure, i.e., porosity, pores connectivity and distribution, but also by the degree of saturation and ionic concentration of the pore solution. Therefore, two different concretes with the same resistivity may have very different microstructures and thereby, different durability related properties. As a result, concrete resistivity may not be a good indicator of concrete transport properties.

On the other hand, FF considers the contribution of the pore solution resistivity to the overall resistivity of the concrete, so that the porous network and transport properties of the concrete can be inferred. FF is inversely proportional to the product of concrete porosity and concrete pore connectivity and directly proportional to the concrete diffusion.

However, the biggest challenge when using FF is determining the pore solution electrical resistivity, as the pore solution needs to be extracted from the concrete for its resistivity to be determined. This extraction requires special equipment and skills, is time-consuming and is normally carried out only for research purposes.

In an effort to streamline the FF calculation, in 2019, ASTM C1876 and later in AASHTO TP 119 (version 2020) proposed immersing the specimens in a designed conditioning solution of Na^+ , K^+ , Ca^{2+} , OH^- , instead of a standard lime-saturated water bath or moist room. This alkaline solution is now the default method for conditioning specimens (DC). It assumes that an equilibrium between pore solution and conditioning solution is achieved, so that the resistivity of the pore solution can be considered the same as the known resistivity of the conditioning solution. The electrical resistivity of the conditioning solution is then used to calculate FF, instead of the experimentally obtained resistivity of the pore solution.

Nevertheless, there are several concerns regarding this type of conditioning, including:

- Does the concrete pore solution really equilibrate with the conditioning solution? If not, what is the impact on the FF?

- The DC does not allow cylinders from different batches to be conditioned together. Consequently, a significant number of separate containers is needed, requiring a large laboratory footprint for storage during testing.
- The DC requires a constant ratio between the volume of concrete specimens and the volume of the conditioning solution. Moreover, since conditioning solutions used in previous tests already contain ions that leached from the other specimens, these solutions should not be reused. Inevitably, State DOTs and the industry are apprehensive regarding the logistics and costs of using large quantities of solution. They are also concerned about the practicality of the proper preparation, handling, and disposal of large quantities of conditioning solution, which has high pH.

3. RESEARCH NEED STATEMENT

There is a need to overcome the practical challenges that FF implementation poses.

4. RESEARCH OBJECTIVES

- Characterize WisDOT mixtures and determine the range of concrete electrical resistivity and pore solution electrical resistivity;
- Evaluate the effect of different conditionings on concrete and pore solution electrical resistivities, as well as in the resulting FF values for WisDOT mixtures;
- Evaluate if equilibrium between conditioning solution and pore solution is reached for WisDOT mixtures;
- Investigate the impact on FF values when equilibrium between pore solution and conditioning solution is not reached;
- Investigate alternative conditioning methods;
- Investigate alternative means to obtain FF for WisDOT mixtures;
- Create a database of pore solution resistivity, bulk resistivity, and FF for WisDOT materials and mixtures.

5. LITERATURE REVIEW

5.1.1.1. Concrete Electrical resistivity

Because of its practicability, concrete electrical resistivity has been used as an indicator of concrete's transport properties by several States, including FDOT, ITD, KDOT, LADOT, MDOT (Montana), MaineDOT, NHDOT, NJDOT, NVDOT, PenDOT, RIDOT and VDOT [5], [6], [7]. Other States, such as IowaDOT, MDOT (Michigan), MNDOT, NCDOT, NYDOT, WisDOT are in the process of implementation or planning to implement concrete electrical resistivity in their specifications.

Several studies have shown different correlations between concrete resistivity and durability related properties. For example, the relationship between surface resistivity and the results of the rapid chloride penetration test (ASTM C1202[8]) vary from study to study, as shown in Figure 1

[6], [9], [10]. The reason for such a difference is not testing age or mixture proportions or materials [10], [11]; some have argued that, instead, it is the specimen-lime-water volume ratio, which affects the leaching of the alkalis [12].

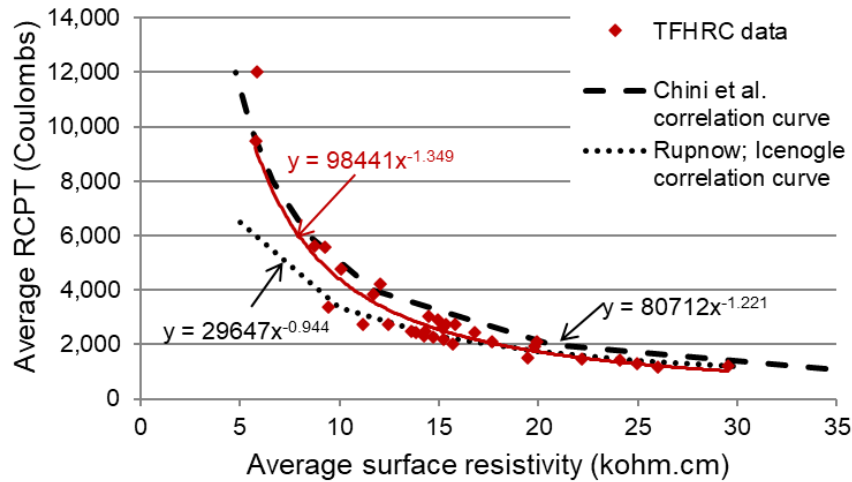


Figure 1 – Relationship between surface resistivity and RCPT in three studies[10].

Although concrete electrical resistivity is related to concrete’s microstructure and durability, by itself, resistivity is not a direct measure of either of them. Rather, it indicates how easily ions move within concrete when an electric field is applied. This movement of ions occurs through the most conductible (lower resistance) phase of a composite material. In the case of concrete, this is the liquid phase in the pores because the electrical conductivity of the solid phases (aggregates, unhydrated and hydrated cementitious materials, as well as vapor phases) are several orders of magnitude lower than that of the pore solution [13].

In summary, concrete electrical resistivity is not a function exclusively of the concrete’s microstructure, i.e., the volume, size, and connectivity of the pores, but it is also related to the pores’ saturation and the ionic concentrations in the pore solution [14]. A schematic representation of the factors affecting resistivity is shown in Figure 2.

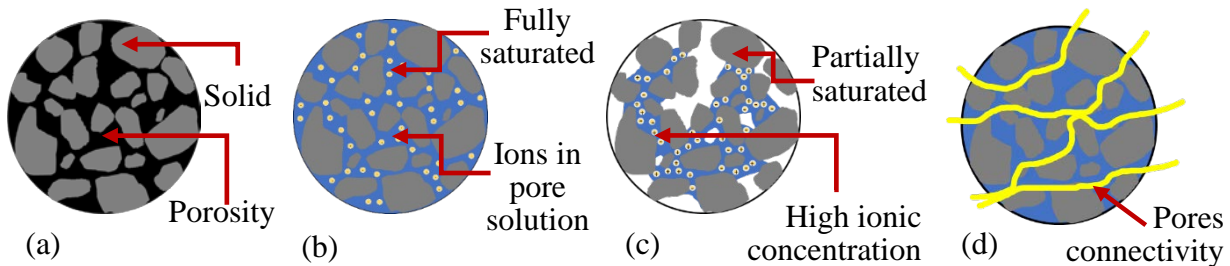


Figure 2 – Factors affecting concrete resistivity; (a) Porosity and solids; (b) saturation, (c) ionic concentration of the pore solution, (d) pores connectivity. (Adapted from Spragg *et al.*[15] and Tanesi *et al.*[16]).

It is intuitive that a higher porosity and a higher pore connectivity will result in lower resistivity, because of the ease of the ionic movement (higher conductivity). Also, the higher the degree of saturation (more water present in the system), the lower the resistivity, provided the ionic concentration is the same.

Because of the role the pore solution plays in the concrete electrical resistivity, two different concretes with the same resistivity may have very different microstructures and thereby durability related properties (Figure 3). Only if one considers the contribution of the pore solution resistivity to the overall measured resistivity of the concrete, the porous network and transport properties of the concrete can be inferred. In order to do so, the concept of formation factor (FF) has been introduced [17].

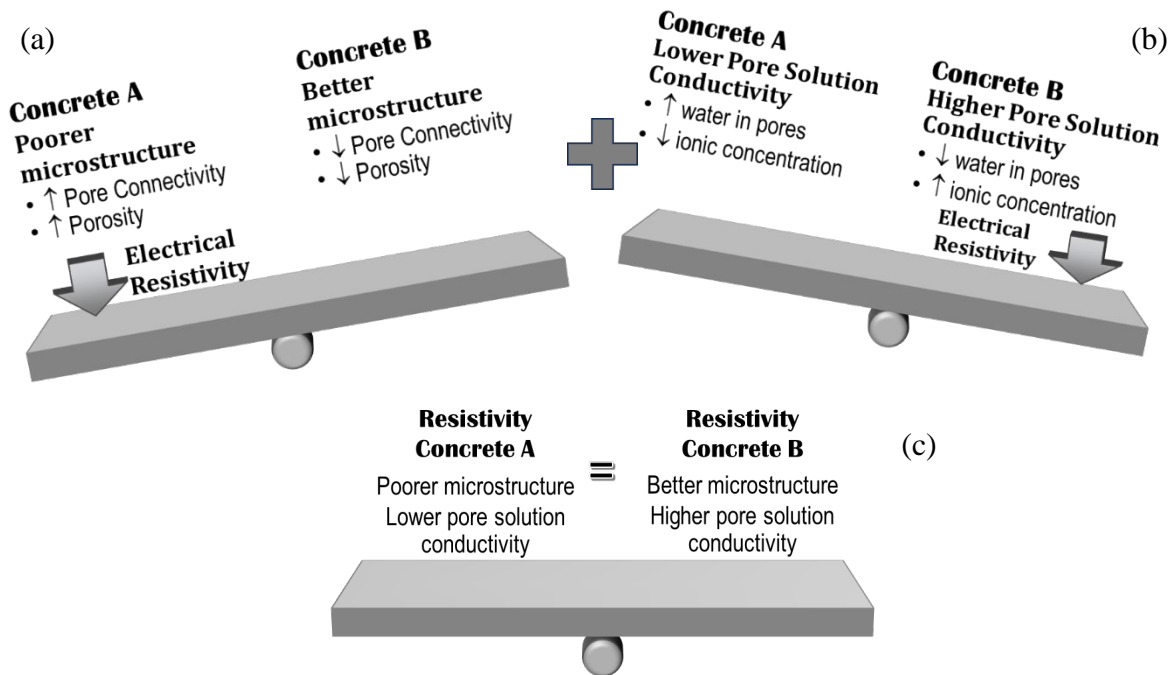


Figure 3 – (a) Poorer concrete microstructure leads to lower concrete resistivity (concrete A), (b) concrete higher degree of saturation and higher ionic concentration of the pore solution lead to lower resistivity (concrete B), (c) combination of microstructure and pore solution result in the same resistivity for concretes A and B [1].

5.1.1.2. Formation Factor

FF, on the other hand, is a fundamental property that provides information on the fluid-filled pore volume and how the fluid-filled pores are interconnected among each other [13]. These parameters are directly related to the concrete's ionic diffusion coefficient, permeability, and water absorption (Equation 1) [2], [11], [16], [17]. Moreover, FF can be implemented in a life cycle assessment to estimate the service life of a concrete structure [18].

AASHTO R 101 [19] (previously known as AASHTO PP 84 [20]) presents performance requirements for transport properties and freeze-thaw resistance as a function of FF of specimens subjected to the DC for 91 days.

Equation 1 shows that FF is calculated by dividing the concrete resistivity by the resistivity of the pore solution. The biggest challenge is determining the pore solution resistivity, as the pore solution needs to be extracted from the concrete. This extraction requires special equipment and skills (Figure 4a), is time-consuming and is normally carried out only for research purposes. After obtaining the pore solution, its resistivity can be directly obtained (Figure 4b) or calculated from the measured ionic concentrations in the pore solution.

$$FF = \frac{\rho}{\rho_0} = \frac{1}{\phi \cdot \beta} = \frac{D_b}{D_0} \quad \text{Equation 1}$$

Where:

FF = Formation factor

ϕ = Concrete porosity

ρ = Concrete resistivity, ($\Omega \cdot m$)

β = Concrete pore connectivity

ρ_0 = Pore solution resistivity, ($\Omega \cdot m$)

D_b = Concrete diffusion coefficient of a defined ion, (m^2/s)

D_0 = self-diffusion coefficient of defined ion, (m^2/s).

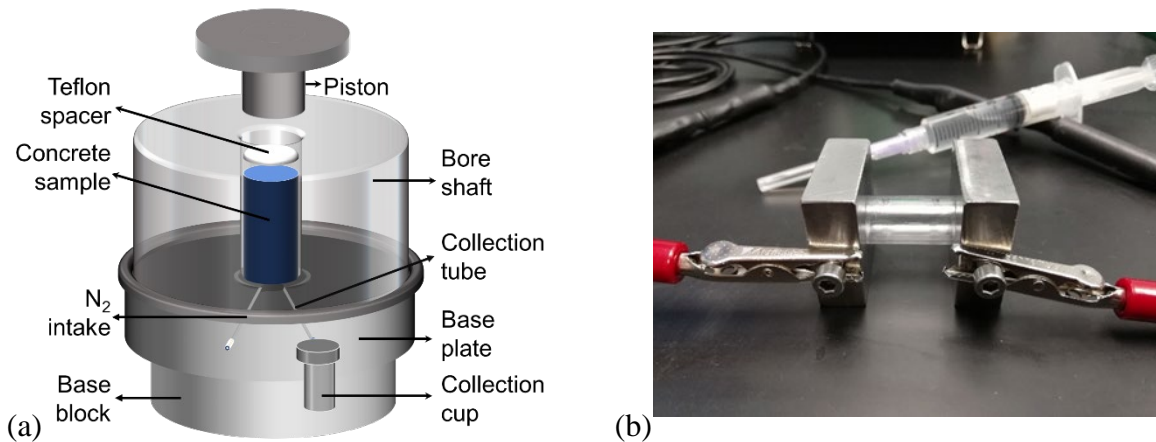


Figure 4 – (a) Schematics of the pore solution expression apparatus; (b) Resistivity cell for pore solution measurements [21].

In an effort to streamline the FF calculation, alternative means to the pore solution expression have been proposed. The first one is the use of mathematical models to estimate the pore solution electrical resistivity.

The most popular one was developed by Bentz *et al.* [22] at National Institute of Science and Technology (NIST), which is a model based on the mixture proportion, the cementitious material's alkali composition, the degree of reaction and a free alkali factor. The default free alkali factor is 75% for portland cement and fly ash, and zero for slag. The model then estimates the K^+ , Na^+ and OH^- concentrations, which are applied to the electrochemical model developed by Snyder *et al.* [23] and calculates the pore solution electrical conductivity, which is the inverse of electrical resistivity.

To assess the performance of the NIST pore solution calculator, literature studies on pore solutions were collected and analyzed [24], [25], [26], [27], [28], [29], [30], [31], [32], [33], [34], [35], [36], [37], [38], [39]. The ionic concentrations reported in the literature studies were input to the electrochemical model developed by Snyder *et al.* [23] to calculate the pore solution electrical resistivity. Simultaneously, the NIST pore solution calculator was used to estimate the pore solution electrical resistivity based on the mixture proportions and the oxide composition provided in literature studies and applying the Snyder *et al.* model [23]. For these estimations, since the age of the pore solution was known from the studies, a model from Parrot and Killoh [40] was adopted to improve the estimation of the age-dependent degree of reaction of the cementitious materials.

Figure 5 compares the NIST calculator estimations with the resistivity calculated from ionic concentrations data in literature. This comparison comprises about 700 mixtures in the literature, out of which 135 were ordinary portland cement mixtures (OPC), 100 were fly ash binary mixtures and 130 were slag cement binary mixtures. Figure 5b shows that the NIST model is not a good predictor of the pore solution resistivity for fly ash mixtures. So, Montanari modified the NIST model. The solver function was applied to the fly ash in order to find the free alkali ion factor value that would minimize the average absolute error on the estimations. The degree of reaction of the system was again estimated with the Parrot and Killoh model [40]. It was found the optimal value stays the same for the cement (0.75) and becomes 0.07 for the fly ashes. These estimations are represented as blue circles in Figure 5b. An overview of this model can be found in Appendix A.

Following the same procedure, the pore solution resistivity was estimated using the NIST calculator for the slag cement. The optimal value for free alkali was found to be equivalent to 0.096. These estimations are represented as blue circles in Figure 5c.

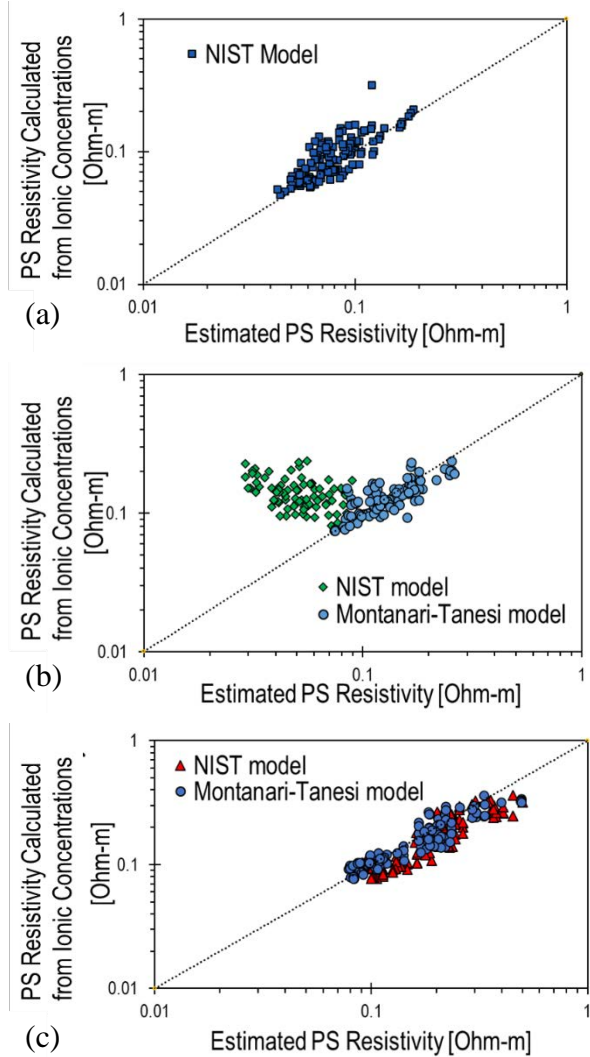


Figure 5 – Pore solution resistivity (a) OPC mixtures, (b) Binary mixtures with fly ashes, and (c) Binary mixtures with slag cement. Values in y-axis were calculated based on the ionic concentrations of species.

Another well-known model to estimate ionic concentration is the Gibbs Energy Minimization Selektor (GEMS). This approach has been vastly used in recent years by the research community [29], [38], [41], but its use has yet to expand to industry, due to the complexity of the required inputs.

Nevertheless, it is important to highlight that these models can only be applied if there is no leaching of ions, i.e., if the concrete is cured in a sealed condition because lime-saturated water only prevents leaching of Ca^{2+} ions, allowing alkalis to leach out from the concrete's pore solution. Consequently, the pore solution concentration (and resistivity of both the pore solution and the concrete) can change significantly. Spragg *et al.* [12] has shown that the pore solution resistivity can change by a factor of four, Montanari *et al.* showed it can change by a factor of two [42].

Moist room storage also promotes leaching due to the water that condenses on the surface of a specimen [12]. Obla and Lobo showed that the pore solution resistivity decreased 78%, while the concrete resistivity decreased 23%, when moist room was used [43]. On the other hand, concrete cured in sealed conditions may cause self-desiccation, affecting the degree of reaction and the resulting microstructure.

In 2019, ASTM C1876 [44], and later in AASHTO TP 119 (version 2020), a second alternative method to expressing pore solution for the calculation of FF was proposed. It consists of immersing the specimens in a designed conditioning solution of Na^+ , K^+ , Ca^{2+} , OH^- , with an electrical resistivity of approximate 0.127 Ohm·m, instead of a standard lime-saturated water bath or moist room. The reason that only NaOH, KOH, and $\text{Ca}(\text{OH})_2$ are used in the conditioning solution is that they are the main contributors to the pore solution electrical conductivity (the inverse of the resistivity) after the sulfate depletion, which typically occurs during the first 24 hours of hydration.

Due to the similar ionic mobility and equivalent conductivity of K^+ and Na^+ ions [23], the respective concentration of the two ions in the conditioning solution are less important than that of the hydroxyl anion (OH^-). This means that K^+ and Na^+ can be combined with different concentrations if the target hydroxyl ion concentration and solution resistivity is obtained.

This is the default conditioning (DC) in AASHTO TP 119 [45] and ASTM C1876. The idea is that after the immersion in the conditioning solution (Figure 6a), the paste pores absorb the conditioning solution (Figure 6b) and the ions diffuse between pore solution and conditioning solution, until the equilibrium between them is reached (Figure 6c). Based on the assumption that such equilibrium is reached, the pore and the conditioning solutions have the same known composition and, consequently, the same electrical resistivity, so the FF is calculated by dividing the concrete resistivity by the resistivity of the conditioning solution.

However, depending on the mixture, previous research has shown that such equilibrium is not reached [42], [43]. The pore solution resistivity, after 56 days of conditioning, varied from 0.147 Ohm·m for a plain cement mixture to 0.163 Ohm·m to a fly ash binary mixture and to a 0.209 Ohm·m to a slag binary mixture. The difference between the FF calculated using the standard conditioning solution resistivity of 0.127 Ohm·m and that calculated using the value obtained from the expressed pore solution varied from 16% for the plain concrete mixture to 46% to the slag binary mixtures.

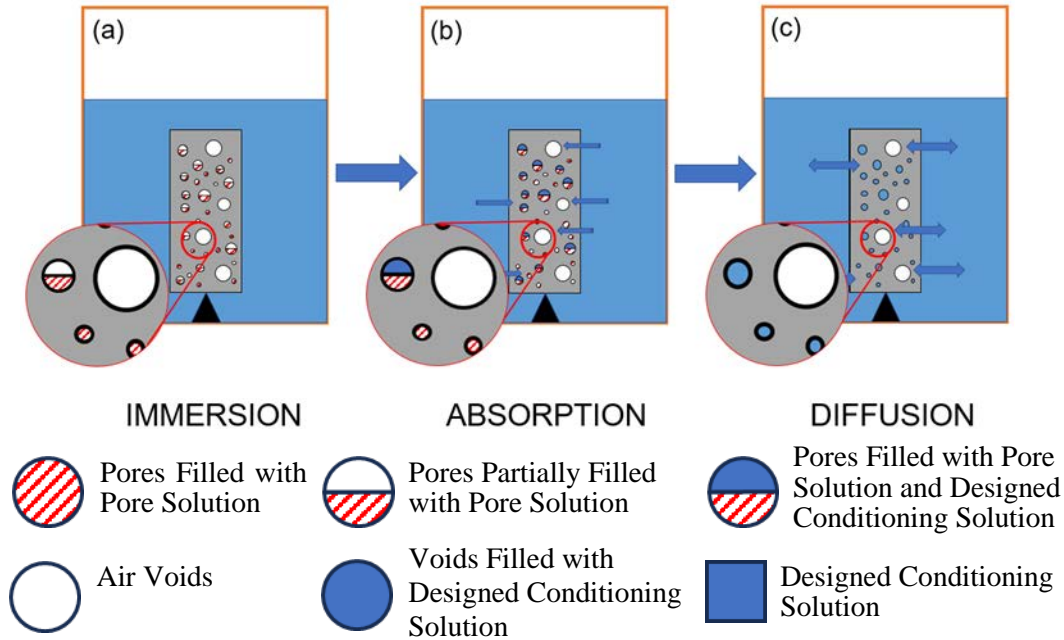


Figure 6 – Schematic of the concentrated alkali conditioning solution procedure on a concrete cylinder specimen. Red-dash dots are gel pores saturated with the mixture’s original pore solution (at the time of specimen immersion); half-red-dash dots are matrix pores partially filled with the original pore solution; red-blue dash dots are matrix pores filled with the alkali-concentrated conditioning solution and partially filled with the original pore solution; blue dots indicate pores filled with the alkali-concentrated conditioning solution; and big white dots represent non-filled entrained air voids.

6. RESEARCH PLAN

6.1. Materials

Five cementitious materials were chosen for the initial evaluation: Alpena Type 1L cement, Continental type 1L cement, Elm Road class C fly ash, Marissa class F fly ash, Ottumwa reclaimed ash, and St Mary’s slag, and three coarse aggregates: a dolomitic limestone from Lannon Stone, a basalt from Earl quarry, and an altered basalt from Dresser Trap Rock. The oxide composition of the cementitious materials was obtained according to ASTM C114 by XRF and available alkalis were determined according to ASTM C311/C311M.

6.2. Phase I – Effect of Conditioning on the Electrical Resistivity and Formation Factor

In Phase I, the effect of three different conditionings or curing (sealed, limewater and C1876 default conditioning) on the resistivity and the FF was studied. Figure 7 gives an overview of Phase I.

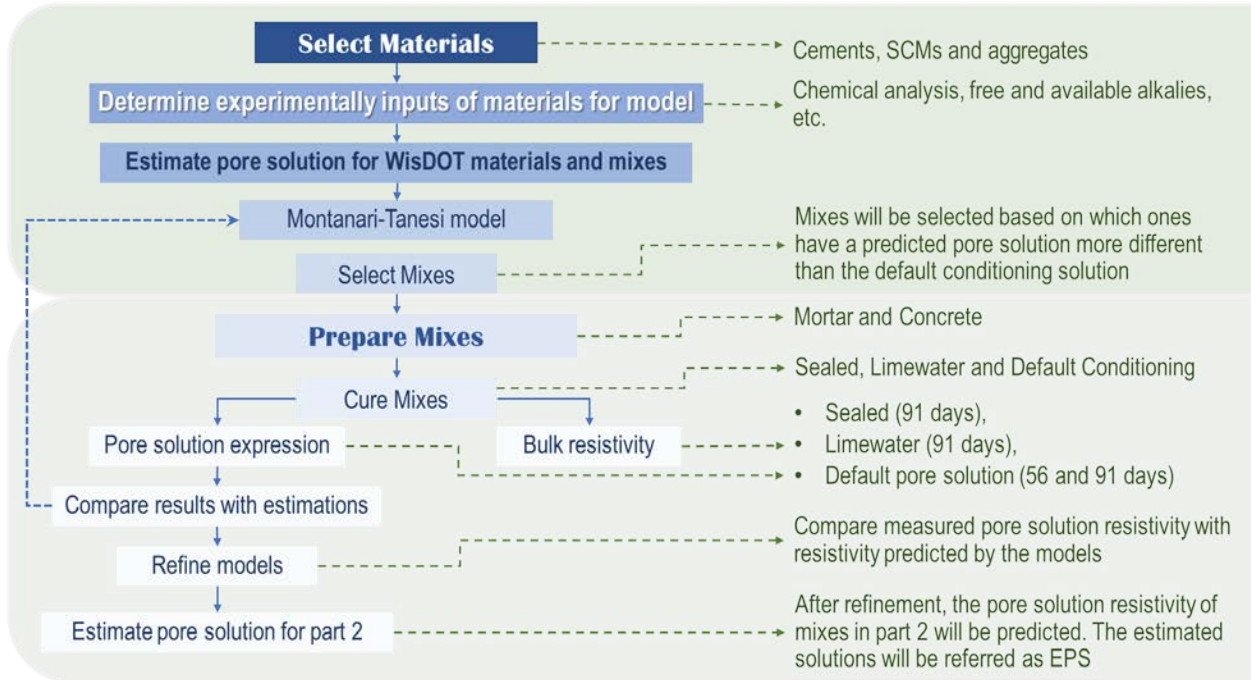


Figure 7 – Project plan for Phase I.

6.2.1. Mixture Selection

A 565 lb/yd³ mixture was used as baseline. Then the modified NIST model (Montanari model) was applied to estimate the pore solution resistivity varying the w/cm between 0.37 to 0.45 and the percent cement replacement from 15% to 30%. A total of 832 iterations (estimations) were performed, according to Figure 8.

The mixtures with an estimated pore solution resistivity that differed the most from the resistivity of the default conditioning, i.e., from 0.127 Ohm·m, were selected for the first phase of batching (Table 1).

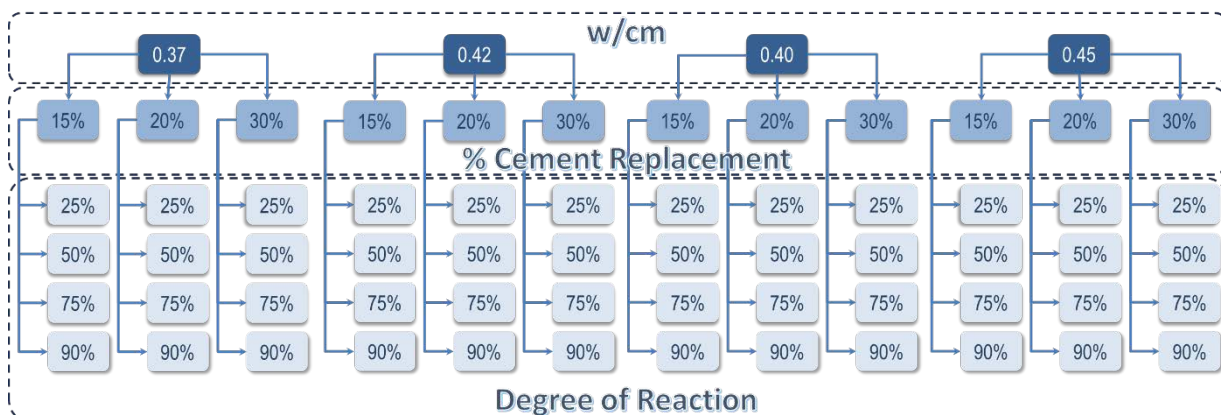


Figure 8 – Variables for the determination of the pore solution resistivity.

Table 1 – Mixture Proportions for Phase I.

	Elm Road	Coal Creek	Slag	Reclaimed Ash
Alpena Cement, lb/yd ³	395	395	395	395
SCM	Elm Road	Coal Creek	Slag	Reclaimed Ash
SCM, lb/yd ³	170	170	170	170
Lannon Stone Coarse agg., lb/yd ³	1,650	1,650	1,650	1,650
Sand, lb/yd ³	1,435	1,430	1,450	1,430
Water, lb/yd ³	254	254	254	254
w/cm	0.45	0.45	0.45	0.45
Polychem Paver Plus, oz/100lb	3.7	3.7	3.7	3.7
MAPEI, oz/100lb	1.0	1.0	1.0	1.0

6.2.2. Phase I - Mixture Preparation and Conditioning

The coarse aggregate was a #67 from Lannon quarry, with 2.77 specific gravity and 0.94% absorption, while the fine aggregate was a natural sand with a 2.66 specific gravity and 0.90% absorption. Alpena Type IL cement was used. The mixture proportions are found in Table 1.

Four concrete mixtures were batched and twenty-seven 4-in by 8-in. concrete cylinders were cast according to ASTM C192 for each mixture or a total of one hundred and eight cylinders. Fresh properties were also determined according to AASHTO T 119M/T 119-23 (slump)[46], unit weight according to AASHTO T 121M/T 121-23 [47], and air according to AASHTO T 395-22 [48]. In addition, nine 2-in by 4-in. paste cylinders were cast for each mixture, according to ASTM C305 for each mixture, or a total of twenty seven paste cylinders. They were conditioned the same way as the concrete cylinders. The slag mixture did not have any paste specimens prepared as all the slag had been used by the time the paste mixtures were prepared.

The cylinders of each mixture were cured or conditioned in three different ways:

Sealed Conditioning (SC): The concrete cylinders were not demolded. The lids were sealed with tape, placed in double bags, and placed in the moist room until they reached testing age.

Limewater Curing (LW): The concrete cylinders were demolded after 24 hours and placed in lime-saturated water, according to ASTM C511, until testing age.

Default Conditioning (DC): The concrete cylinders were demolded after 24 hours and placed in the simulated pore solution, as specified in ASTM C1876, until testing age.

6.2.3. Phase I - Testing

Bulk resistivity according to ASTM C1876 was performed at ages 28, 56 and 91 days on three specimens per age. The compressive strength at 28 days was determined on specimens cured in limewater.

In order to calculate FF, the pore solution resistivity was determined by different means (Figure 9).

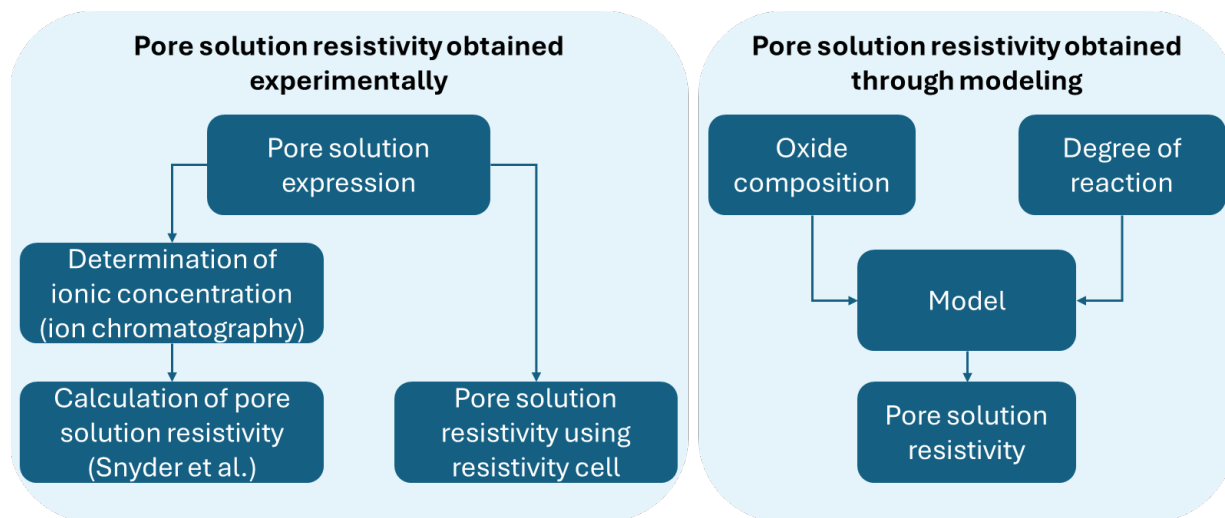


Figure 9 – Determination of the pore solution resistivity.

6.2.3.1. Pore Solution Expression

At the testing age, the concrete specimens were first split into two with a compression machine, similar to the ASTM C496, procedure, but with a loading rate to approximately 2450 N/s. One half of the split cylinder was then divided into two quarters by using the sharp edge of a geological hammer. The cylinders' quarters were crushed with a modified electrical hammer (equipped with a 65-mm-diameter flat head and sieved through a 3/8-in. sieve, then transferred into the expression apparatus for testing. This procedure followed Montanari *et al.* [21].

Pore solution was expressed from the concrete using an apparatus similar to the one used by Montanari *et al.* [21]. The maximum normal pressure applied was at a loading rate of 551 lbf/s (174 psi/s). Then, the maximum load was maintained for 3 min, after which the entire load was instantly removed.

After being expressed, the pore solutions were frozen to minimize the potential for evaporation and carbonation of the ionic species. Afterwards, each frozen pore solution was thawed, and its ionic concentration or resistivity were determined experimentally.

6.2.3.2. Ionic Concentration

The ionic concentration of the pore solution of some of the samples was measured by ion chromatography.

6.2.3.3. Calculation of the Resistivity of the Expressed Pore Solution from the Dissolved Alkalis

The electrical resistivity was calculated from the ionic concentration using the Snyder *et al.* model [23].

6.2.3.4. Pore Solution Electrical Resistivity

The solution was moved to a syringe and let rest until the temperature reached 75 ± 2 °F. Then, the pore solution was injected into the polycarbonate tube and impedance and phase angle were obtained using a resistivity cell connected to an impedance meter. Then, resistivity was calculated according to Equation 2.

The procedure followed what is described in Montanari *et al.* [21]. The cell used is shown in Figure 10.

$$\rho_0 = Z \times \cos(\text{radians}(\theta)/180) \times k \quad \text{Equation 2}$$

Where:

Z = impedance

k = geometric factor

θ = phase angle

The geometric factor for the cell was calculated according to Equation 3.

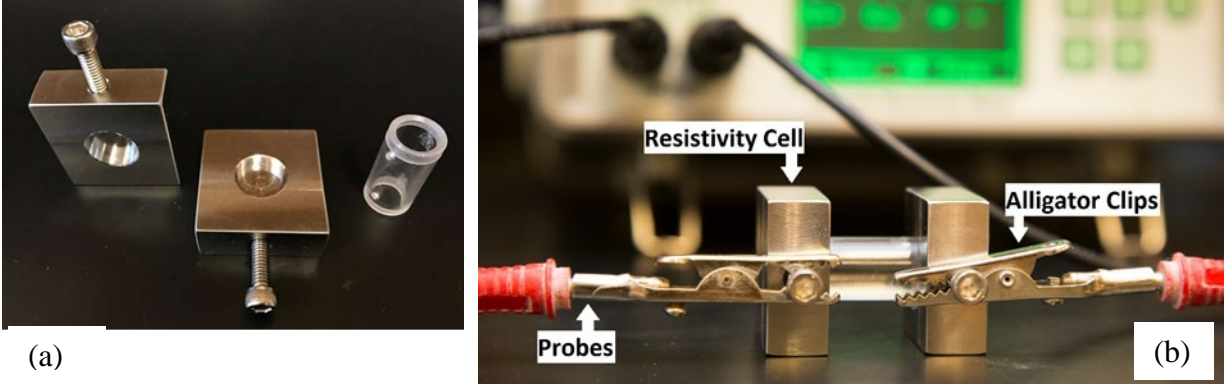
$$k = \frac{A}{L} \quad \text{Equation 3}$$

Where:

k = geometric factor

L = length of the polycarbonate tube

A = cross-sectional area of the polycarbonate tube



Stainless Steel Plates of Resistivity Cell



Polycarbonate Tube of Resistivity Cell

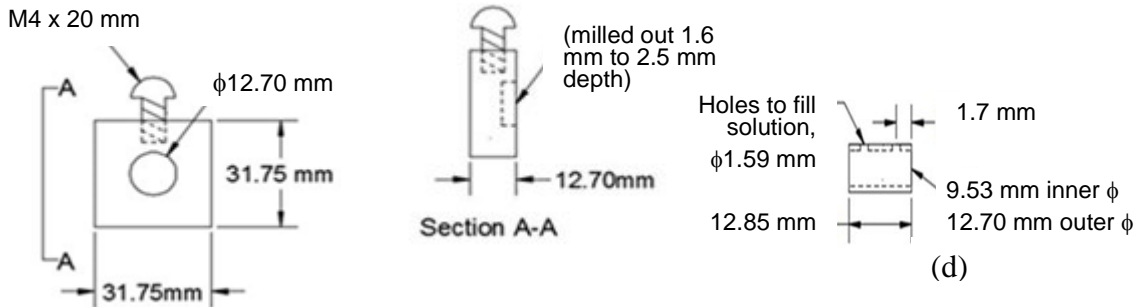


Figure 10 – Pore solution resistivity. (a) resistivity cell, (b) resistivity set up, (c) dimensions of the stainless-steel plates of the resistivity cells, and (d) dimensions of the polycarbonate tube of the resistivity cell.

6.2.3.5. Degree of Reaction

The degree of reaction is an input for the NIST model. The paste cylinders were crushed and Thermogravimetry Analysis (TGA) was performed to obtain non-evaporable water.

The degree of reaction calculation was based on the non-evaporable water [49], [50], [51]. The methodology was proposed by Meziani *et al.* [52]. The non evaporable water is calculated according to Equation 4.

$$W_n = L_{dh} + L_{dx} + 0.41 \times (L_{dc} - L_{dca}) \quad \text{Equation 4}$$

Where:

$W_n(\%)$ = Amount of non-evaporable water

$L_{dh}(\%)$ = Mass loss between 105 °C and 400 °C due to the dehydration of the hydrates

$L_{dx}(\%)$ = Mass loss between 400 °C and 600 °C due to the dihydroxylation of calcium hydroxide

$L_{dc}(\%)$ = Mass loss between 600 °C and 800 °C due to the decarbonation of calcite

$L_{dca}(\%)$ = Mass loss between 600 °C and 800 °C/ mass at 105 °C due to the decarbonation of anhydrous samples

$$w_{\infty} = \frac{w_n \times (t + k)}{t} \quad \text{Equation 5}$$

Where:

k = constant

t = time in hours

The degree of hydration is calculated according to Equation 6:

$$\alpha = \frac{w_n}{w_{\infty}} \times 100 \quad \text{Equation 6}$$

Where:

$W_n(\%)$ = Amount of non-evaporable water at a specific age, in this study 56 days.

$w_{\infty}(\%)$ = Amount of non-evaporable water at full hydration.

6.2.3.6. Porosity

In order to determine if the different conditionings had an effect on the microstructure of the concrete, the porosity of paste cylinders was determined using mercury intrusion porosimetry. The pore size distribution and porosity analysis of the sample(s) was conducted on a mercury intrusion porosimeter with a working range of approximately 1 psia to 60,000 psia or approximately 0.004 μm to 200 μm . The instrument measured the volume of mercury, a non-wetting liquid, as it intrudes into a sample at increasing pressures to probe increasingly smaller pores. The Washburn equation was used to calculate the inner equivalent cylindrical pore diameter based on the pressure applied. Other parameters can then be derived.

It should be noted that mercury fills the interstices between particles (interparticle voids) as well as pores within particles (intraparticle voids). Closed pores cannot be measured by this technique as they are inaccessible to mercury. Results reported over the entire analytical range include both intra-particle and inter-particle void spaces.

6.3. Phase 2 – Mixtures' Preparation and Testing

The second phase of concrete batching consisted of modifying the mixtures or conditionings from the first phase and assessing their effect on the concrete electrical resistivity and formation factor.

6.3.1. Phase II - Mixture Preparation and Conditioning

In this phase, a total of fifteen mixtures were prepared and two hundred and fifty 4-in. by 8 in. cylinders were cast, according to ASTM C192. Fresh properties were determined according to AASHTO T 119M/T 119-23 (slump)[46], unit weight according to AASHTO T 121M/T 121-23 [47], and air according to AASHTO T 395-22 [48].

Compressive strength at 28 days in LW curing was determined according to AASHTO T 22M/T 22-22[53], and bulk resistivity according to ASTM C1876-24[44].

In Phase II, surface resistivity was determined according to WTM T358[54], a WisDOT modified version of AASHTO T 358-22[55], with the exception of the correction factor, since specimens were 4-in. by 8 in. cylinders. The calculation of surface resistivity is shown in Equation 7.

$$Sr = Sr_{T358} \times Cond. \times 0.512 \quad \text{Equation 7}$$

Where:

Sr = surface resistivity

Sr_{T358} = apparent surface resistivity determined according to AASHTO T 358

Cond = correction factor for conditioning. 1.1 for LW, DC and EPS, 1.05 for PS2 and 1.0 for AC

0.512 = geometric correction factor for 4 by 8 in. cylinders

Additionally, in phase II, chloride penetrability was determined according to ASTM C1202-22e1 (RCPT). Table 2 presents the acronyms for the conditionings used in Phase II.

Table 2 – Conditioning Acronyms.

LW	Limewater: cylinders were cast and demolded after 24 hours and placed in lime-saturated water, according to ASTM C511 until time of testing.
DC	Default conditioning: cylinders were cast and demolded after 24 hours and placed in simulated pore solution saturated with calcium hydroxide, according to ASTM C1876 until time of testing.
EPS	Estimated pore solution: the resistivity of the pore solution of each mixture was estimated using the Montanari model and a solution with the same resistivity was prepared. Cylinders were cast and demolded after 24 hours and placed in the EPS until time of testing.
AC	Accelerated curing: cylinders were cast and demolded after 24 hours and placed in limewater until age of 7 days at 73 ± 3 °F until age of 7 days. Then, the temperature increased to 100 ± 3 °F, until the age of 28 days.
SL	Sealed: cylinders were not demolded. The lids were sealed with tape, placed in double bags, and placed in the moist room until time of testing.

Pore Solution 2: the average of the pore solution resistivity of the sealed specimens of all mixtures of Phase I was calculated. A solution with composition of 111.29 g NaOH, 66.91 g of KOH and 6.9 g of Ca(OH)₂ reflecting this electrical resistivity was prepared and used as conditioning solution 2. Cylinders were cast and demolded after 24 hours and placed in this solution until time of testing.

6.3.2. Effect of Coarse Aggregate

From phase 1 of concrete testing, the Elm Road mixture was chosen as baseline. Then the coarse aggregate was replaced either by Earl quarry or by Dresser Trap Rock (Figure 11).

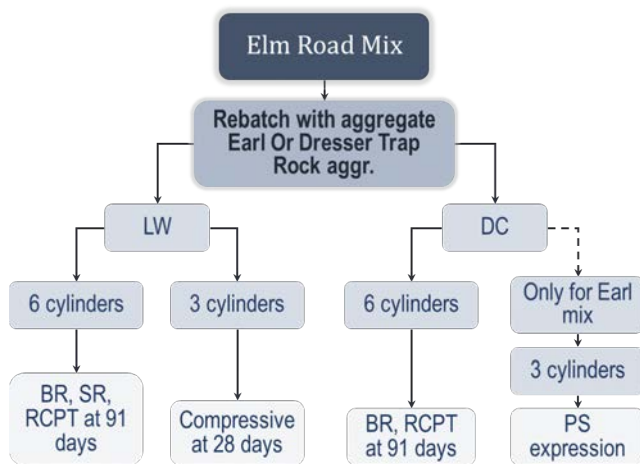


Figure 11 – Influence of aggregates testing matrix. BR stands for bulk resistivity (ASTM C1876), SR stands for surface resistivity (WTM T358), RCPT stands for rapid chloride penetrability test (ASTM C1202), and PS stands for pore solution.

- LW: At 28 days, three cylinders were tested according to ASTM C39/C39M. At 91 days, three cylinders were tested according to ASTM C1876, three cylinders according to ASTM C1202, and three cylinders according to WTM T358.

- DC: At 91 days, six cylinders were tested according to ASTM C1876, and ASTM C1202. For the mixture containing Earl aggregate, three extra cylinders were cast, pore solution was expressed at 91 days and the solution resistivity determined.

6.3.3. Effect of w/cm

From phase 1, Elm Road and Coal Creek mixtures were prepared with a w/cm = 0.37, instead of 0.45. Each of the mixtures was conditioned and tested as follows (Figure 12):

- LW: At 28 days, three cylinders were tested according to ASTM C39/C39M. At 91 days, three cylinders were tested according to ASTM C1876, ASTM C1202, WTM T358.
- DC: At an age of 91 days, three cylinders were tested according to ASTM C1876.
- Estimated Pore Solution (EPS): At the age of 56 days, three cylinders were tested according to ASTM C1876. At the age of 91 days, three cylinders were tested ASTM C1876, ASTM C1202, and WTM T358.

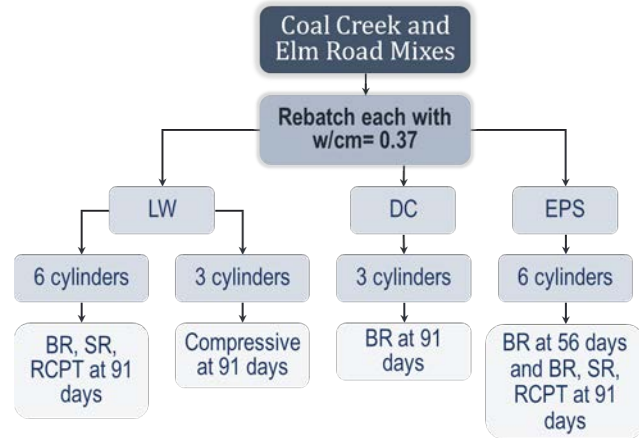


Figure 12 – Influence of w/cm testing matrix. BR stands for bulk resistivity (ASTM C1876), SR stands for surface resistivity (WTM T358), and RCPT stands for rapid chloride penetrability test (ASTM C1202).

To determine the estimated pore solution composition, first the Montanari model was applied to estimate the resistivity of the pore solution for each mixture. Then, using the Snyder *et al.*[23] model, the proportions of each ingredient were determined to result in the required solution resistivity. The Coal Creek mixture, used 254.38 g of NaOH, 141.24 g of KOH and 6.9 g of Ca (CO)₂ in 13.25 L of distilled water and the Elm Road mixture used 185.50 g of NaOH, 111.51 g of KOH and 6.9 g of Ca(CO)₂. The estimated resistivity of the pore solutions were 0.076 ohm-m and 0.097 ohm-m for Coal Creek and Elm Road respectively.

6.3.4. Effect of Cement Replacement

From phase 1, Coal Creek, Elm Road and Slag mixtures were chosen as baseline. Each of the mixtures was prepared with 15% cement replacement, instead of 30%. Each of the mixtures was conditioned and tested as follows (Figure 13):

- LW: At 28 days, three cylinders were tested according to ASTM C39/C39M. At 91 days, three were tested according to ASTM C1876, ASTM C1202, and WTM T358.
- DC: At 56 and 91 days, three were tested according to ASTM C1876. For the Coal Creek and Elm Road mixtures, three additional cylinders were cast, pore solution was expressed and the pore solution resistivity determined.

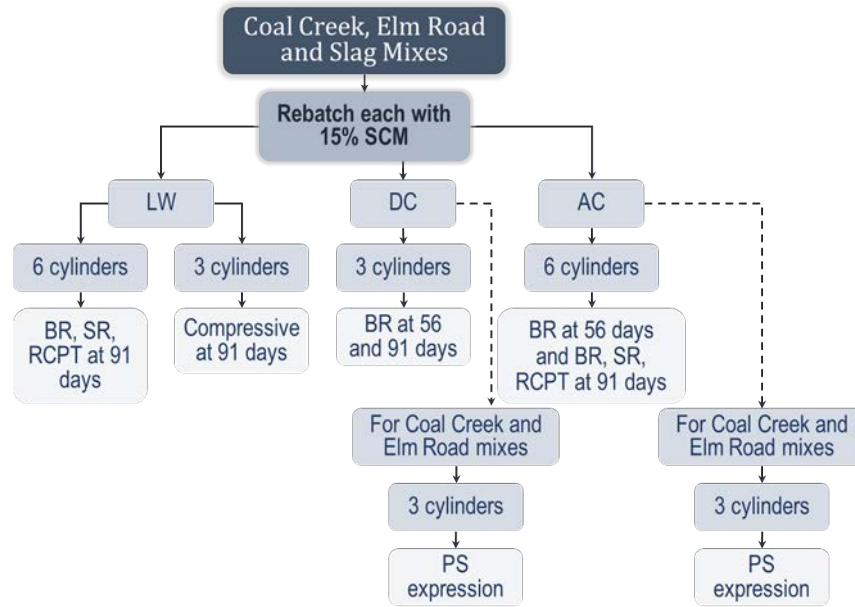


Figure 13 – Influence of cement replacement testing matrix. BR stands for bulk resistivity (ASTM C1876), SR stands for surface resistivity (WTM T358), RCPT stands for rapid chloride penetrability test (ASTM C1202), and PS stands for pore solution.

- Accelerated Curing (AC): Three cylinders were tested according to ASTM C1876, ASTM C1202 and WTM T358.

Additionally, for the Elm Road and Coal Creek mixtures, at an age of 91 days, two cylinders had pore solution expressed, and the solution resistivities determined.

6.3.5. Effect of Cement

From phase 1, the same four mixtures were prepared but the cement was replaced by the Continental cement. Each of the mixtures was conditioned and tested as follows (Figure 14).

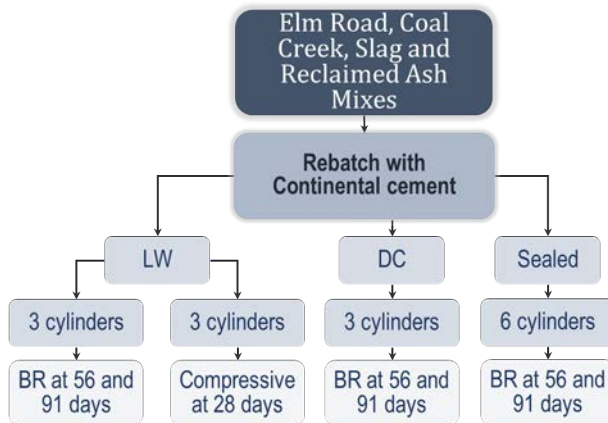


Figure 14 – Influence of cement testing matrix. BR stands for bulk resistivity (ASTM C1876), and RCPT stands for rapid chloride penetrability test (ASTM C1202).

- LW: At 28 days, three cylinders were tested according to ASTM C39/C39M. At 56 and 91 days, three cylinders were tested according to ASTM C1876.
- DC: At the age of 56 and 91 days, three cylinders were tested according to ASTM C1876.
- Sealed: At 56 and 91 days, three cylinders were demolded and tested according to ASTM C1876.

6.3.6. Effect of Conditioning

From phase 1 of concrete testing, all the mixtures were rebatched but exposed to different conditioning regimes. Each of the mixtures was conditioned and tested as follows (Figure 15):

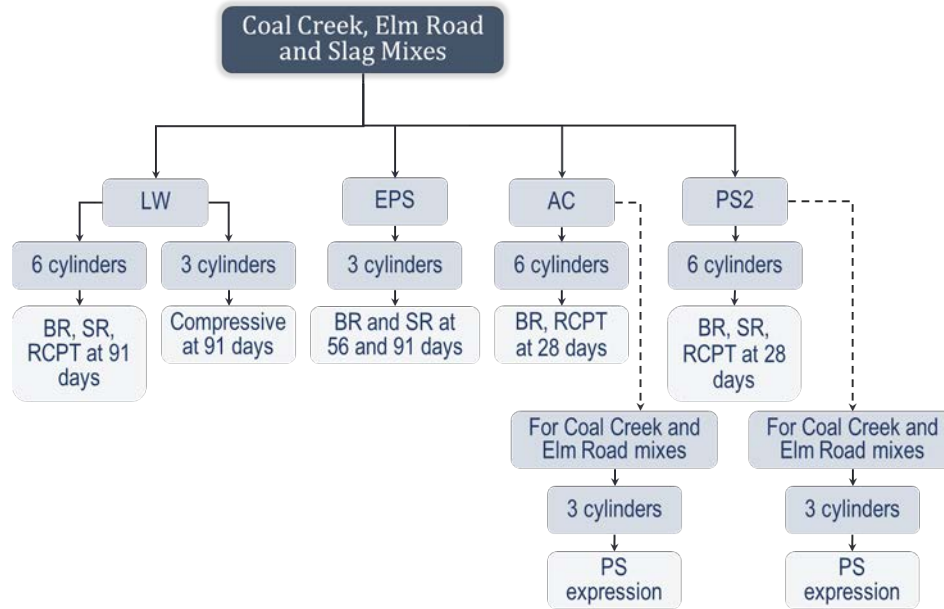


Figure 15 – Influence of SCM testing matrix. BR stands for bulk resistivity (ASTM C1876), SR stands for surface resistivity (WTM T358), RCPT stands for rapid chloride penetrability test (ASTM C1202), and PS stands for pore solution.

- LW: At 28 days, three cylinders were tested according to ASTM C39/C39M. At 91 days, and three were tested according to ASTM C1876, ASTM C1202, and WTM T358.
- EPS: At ages of 56 days and 91 days, three cylinders were tested according to ASTM C1876. The estimated pore solution composition, first the Montanari model was applied to estimate the resistivity of the pore solution for each mixture. Then, using the Snyder *et al.*[23] model, the proportions of each ingredient was determined to result in the required solution resistivity. The solution proportions are below (per 13.25 L):

	NaOH, g	KOH, g	Ca (CO) ₂ , g	Resistivity, oh-m
Coal Creek	164.29	74.34	6.9	0.118
Elm Road	123.48	72.85	6.9	0.142
Slag	68.36	56.50	6.9	0.213

- Accelerated Curing (AC): Six cylinders were tested according to ASTM C1876 and ASTM C1202.
- Pore Solution 2 (PS2): At an age of 56 days, three cylinders were tested according to ASTM C1876. At an age of 91 days, the same three cylinders were tested according to ASTM C1876, followed by WTM T358. Then, they were tested according to ASTM C1202.

Additionally, for the Coal Creek and Elm Road mixtures, conditioned in accelerated conditions or in PS2, at an age of 91 days, three cylinders had pore solution expressed, and the solution resistivity was determined.

7. RESULTS

7.1. Materials' Testing

Table 3 and Table 4 present the chemical composition of the cements and SCMs, respectively.

Table 3 – Chemical Composition of Cements.

Chemical Composition, % mass	Alpena	Continental
Silicon as (SiO ₂)	19.81	19.05
Aluminum as (Al ₂ O ₃)	4.37	4.52
Iron as (Fe ₂ O ₃)	2.62	2.99
Sulfur as (SO ₃)	2.44	3.47
Calcium as (CaO)	63.85	62.53
Magnesium as (MgO)	2.74	2.16
Sodium as (Na ₂ O)	0.16	0.11
Potassium as (K ₂ O)	0.47	0.60
Total Alkali as (Na ₂ O _e)	0.47	0.50
Titanium as (TiO ₂)	0.20	0.21
Phosphorus as (P ₂ O ₅)	0.08	0.12
Zinc as (ZnO)	<0.01	0.07
Manganese as (Mn ₂ O ₃)	0.08	0.46
Chromium as (Cr ₂ O ₃)	<0.01	<0.01
Strontium as (SrO)	0.06	0.04
Loss on Ignition (LOI)	3.34	3.44

Table 4 – Chemical Composition of SCMs.

Chemical Composition, % mass	Elm Road	Coal Creek	Reclaimed Ash	St. Mary's Slag
Silicon as (SiO ₂)	39.46	50.96	33.83	33.25
Aluminum as (Al ₂ O ₃)	19.69	15.69	19.27	13.53
Iron as (Fe ₂ O ₃)	9.54	5.74	5.52	0.82
SUM (SiO ₂ + Al ₂ O ₃ + Fe ₂ O ₃)	68.69	72.39	58.62	-
Sulfur as (SO ₃)	2.16	0.78	1.56	1.8
Calcium as (CaO)	18.21	14.64	22.4	42.9
Sulfide Sulfur (S)	-	-	-	0.47
Magnesium as (MgO)	4.2	4.2	4.1	6.12
Sodium as (Na ₂ O)	1.37	4.03	2.62	0.22
Potassium as (K ₂ O)	0.89	2.18	0.48	0.41
Total Alkali as (Na ₂ O _e)	1.96	5.46	2.94	-
Moisture Content:	0.06	0.09	2.53	-
Loss on Ignition (LOI)	0.65	0.27	5.38	0.62

7.2. Phase 1 Testing

7.2.1. Bulk Resistivity

Figure 16 show the bulk resistivity of the different mixtures over time. The resistivity increase over time for Coal Creek was more pronounced than for the other three mixtures.

A one factor Analysis of Variance (ANOVA) test followed by a Tukey Honestly Significant Difference (HSD) with a 95% confidence was performed.

For the specimens conditioned in limewater, at 28 days, Elm Road presented the highest resistivity, at 56 days Coal Creek and Elm Road are statistically the same, and at 91 days, Coal Creek presented the highest resistivity. This clearly shows that due to different hydration kinetics, the comparison among mixtures can be misleading, depending on the age. Reclaimed Ash presented the lowest at all ages.

For the specimens in default conditioning, at 28 days, slag showed the highest resistivity. At 56 and 91 days, Coal Creek showed statistically the highest resistivity, while Reclaimed Ash showed always the lowest.

For the sealed specimens, at 28 and 56 days, Slag and Elm Road had statistically the same resistivity. At 56 and 91 days, Coal Creek showed the highest resistivity, followed by Elm Road. Reclaimed Ash showed the lowest resistivity at all ages.

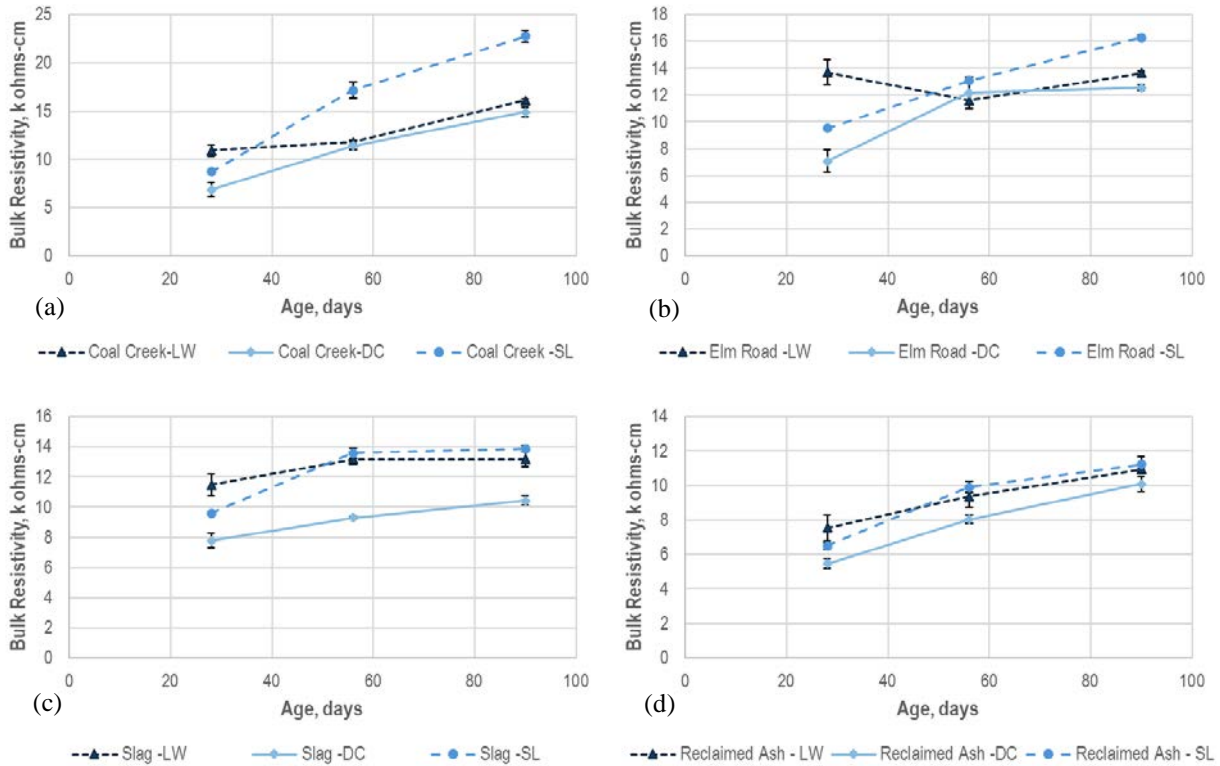


Figure 16 –Bulk resistivity over time for (a) Coal creek mixture, (b) Elm Road mixture, (c) Slag mixture, and (d) Reclaimed Ash mixture. LW stands for limewater, DC for default conditioning (pore solution), and SL for sealed. Error bars indicate ± 1 standard deviation.

In terms of conditionings, at 28 days, the different conditionings yielded statistically different resistivities for all mixtures, except for reclaimed ash.

At 56 days, for the Coal Creek mixture, the resistivity of the specimens in limewater was statistically the same as those in default conditioning. For the Elm Road mixture, there was no statistical difference in resistivity among the different conditionings, while for the Slag and Reclaimed Ash mixtures, the resistivity of the limewater specimens was statistically the same as those sealed.

At 91 days, the effect of conditioning changed again. For Coal Creek, the resistivity of the limewater and the default conditioning were statistically the same, for Elm Road each conditioning yielded statistically different resistivity from each other, for Slag the resistivity of the limewater specimens was statistically the same as those sealed, and for the Reclaimed Ash, the only statistically different resistivities were the ones for default conditioning compared to those sealed.

It is clear that the effect of conditioning varies from mixture to mixture and from age to age. However, in most cases, conditioning played a role in the bulk resistivity. As a trend, the specimens

in default conditioning tended to show the lowest resistivity. At 28 days, limewater tended to show the highest due to leaching of alkalis, but at 91 days, the sealed specimens tended to show the highest, probably due to the self-desiccation of the specimens. A previous study [56] showed that the degree of saturation at 56 days for limewater cured specimens was 80%, while for sealed specimens it was 63%. Despite the self-desiccation, sealed may be more realistic of field conditions, since it is unlikely the pavement will be saturated most of the time. In addition, sealed is the only conditioning that allows the pore solution resistivity to be estimated. Both at 56 and 91 days, limewater and sealed conditionings were more effective in differentiating the mixtures, i.e., the different SCMs resulted in different resistivities.

Table 5 shows the ratio between the default conditioning and limewater bulk resistivities and the sealed and limewater bulk resistivities. With exception of Elm Road, it is clear that the BR_{DC}/BR_{LW} resistivities increase with age. At 91 days, the ratio seems to be around 92% for the fly ashes and 79% for the slag. For BR_{sealed}/BR_{LW} , the ratio increase seems to occur only between 28 and 56 days and then stabilizes. The ratio at 91 days seems to be different for each mixture.

Table 5 – Ratio of Bulk Resistivities.

	BR_{DC}/BR_{LW}			BR_{sealed}/BR_{LW}		
	28 days	56 days	91 days	28 days	56 days	91 days
Coal Creek	63%	97%	93%	80%	146%	141%
Elm Road	52%	105%	92%	69%	113%	119%
Slag	68%	71%	79%	84%	103%	105%
Reclaimed Ash	73%	86%	92%	86%	106%	103%

7.2.2. Pore Solution Resistivity obtained through Modeling

In order to refine the modified NIST model (Montanari model) for the determination of the pore solution resistivity, it was necessary to first determine the degree of reaction (DOR) of the mixtures. Although only the sealed conditioning was needed for the model, DOR was obtained in pastes at 56, and 180 days and subjected to the same conditioning conditions as the concrete (Table 6). Due to unavailability of slag, the DOR of the slag mixture was not determined.

Table 5 shows that for Coal Creek and Elm Road, the DOR varies with the conditioning. This suggests that conditioning procedure might have an impact on kinetics of the reactions and possibly on the microstructure. Table 5 also shows that the DOR increases with time, which was expected.

The Montanari model was refined using the data obtained in this study. For fly ash mixtures, the free alkali ion factor value for the cement was found to be 0.77 and for the fly ash 0. Since there was only one slag mixture, it was not possible to refine the model for slag mixtures.

Table 6 – Degree of Reaction

		Degree of Reaction, %		
		Sealed	Limewater	Default Conditioning
Coal Creek	56 days	89.8	91.3	93.9
	180 days	96.6	97.1	98.0
Elm Road	56 days	95.1	100	75.2
	180 days	98.4	100	90.7
Reclaimed Ash	56 days	100	100	100
	180 days	100	100	100

7.2.3. Pore Solution Electrical Resistivity Obtained Experimentally

Figure 17 presents the pore solution resistivity obtained experimentally and estimated by the revised Montanari model. Figure 17 shows the effect of different conditionings on the resistivity of the pore solution. The resistivity obtained using IC was similar to the resistivity obtained using the resistivity cell, indicating the two methods can be used interchangeably. The Montanari model seemed to overestimate the pore solution resistivity of the Coal Creek mixture and underestimate the one for the Slag mixture. For the Elm Road and Reclaimed Ash mixtures, the model estimation was close to the resistivity obtained experimentally.

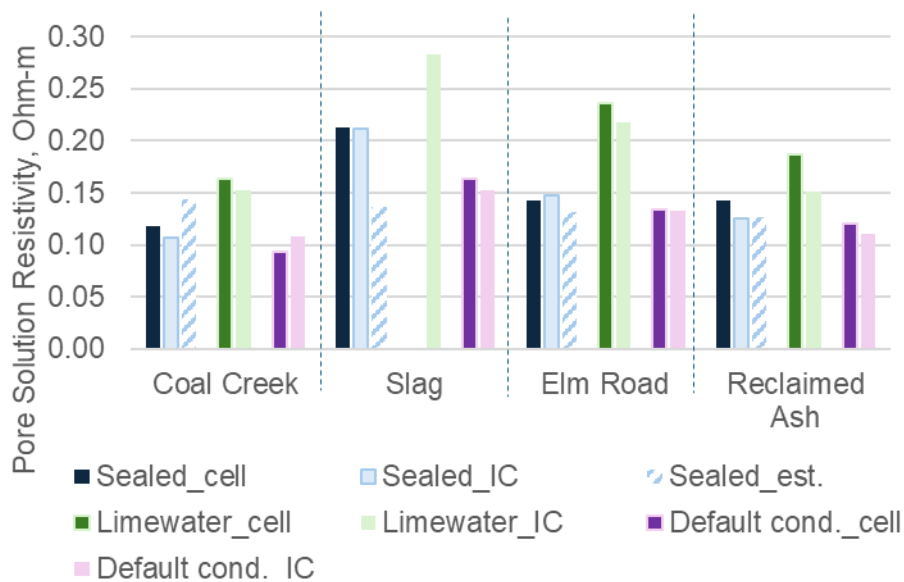


Figure 17 – Pore solution resistivity obtained using the resistivity cell, by determining the chemical composition by ion chromatography (IC) and then calculating the pore solution resistivity (Snyder *et al.* [23]) or estimated by the revised Montanari model. Pore solution resistivity was determined at 91 days for limewater and default conditioning, and at 56 days for sealed condition.

For all the mixtures, the pore solution resistivity was the highest for specimens conditioned in limewater due to leaching. The pore solution of specimens in default conditioning tended to be the lowest. When comparing the different mixtures, the resistivity of the pore solution of the Slag was the highest, and Coal Creek the lowest.

For the default conditioning, the pore solution obtained experimentally was significantly different than the default value of 0.127 ohm-m for the Coal Creek and Slag mixtures, indicating that the equilibrium between the pore solution and the conditioning solution was not achieved. For the Reclaimed Ash mixture the pore solution resistivity was about the same as the default value and for the Elm Road mixture, it was slightly higher than the default value. Equilibrium between the pore solution and the conditioning solution for these mixture might have been achieved.

For fly ash mixtures, the three methods of obtaining the pore solution resistivity yielded comparable results, showing the validity of all of them, confirming the findings of an earlier study [21].

7.2.4. Porosity

Table 7 presents the median pore diameter and the total porosity for selected mixtures conditioned three different ways: sealed, limewater and default conditioning. The pore size and the total porosity of the Coal Creek mixture is considered different among the three conditionings. This means that the conditioning affected the microstructure of the paste. For the Elm Road mixture, the porosity of the limewater and the default conditioning samples can be considered similar, but the pore sizes are considered different among the three conditionings. For the Reclaimed Ash mixture, the pore size of the default conditioning and the sealed samples is the same. The porosity of the sealed and the limewater samples are also considered the same. Overall, the effect of the conditioning on the porosity and pore size depends on the mixture.

Table 7 – Porosity.

	Total Pore Area, m ² /g	Median Pore Diameter, μm	Porosity, %
Elm Road Sealed	35.47	0.02106	23.0
Elm Road LW	38.62	0.01655	21.2
Elm Road DC	32.97	0.01924	21.4
Reclaimed Ash Sealed	60.79	0.01537	32.2
Reclaimed Ash LW	75.88	0.01405	33.8
Reclaimed Ash DC	77.43	0.01557	35.3
Coal Creek Sealed	32.20	0.02326	21.5
Coal Creek LW	45.28	0.02007	26.3
Coal Creek DC	57.60	0.02269	34.7
LW- limewater		DC – default conditioning	

7.2.5. Formation Factor

Figure 18 presents the formation factor calculated based on four different pore solution resistivities:

Cell: bulk resistivity divided by the resistivity of the pore solution that was obtained by using the cell (Figure 10a),

IC: bulk resistivity divided by the resistivity of the pore solution that was determined by calculating the resistivity (Snyder *et al.* [23]) based on chemical composition obtained with IC measurements,

Def.: bulk resistivity divided by the default value of the resistivity of the simulated pore solution, i.e., 0.127 ohm-m.

Est: bulk resistivity divided by the resistivity of the pore solution estimated by using the revised Montanari model.

The horizontal lines indicate AASHTO R 101 requirement for mixtures that are not exposed to freezing and thawing (≥ 500) and mixtures exposed to freezing and thawing and deicing salts ($\geq 1,000$).

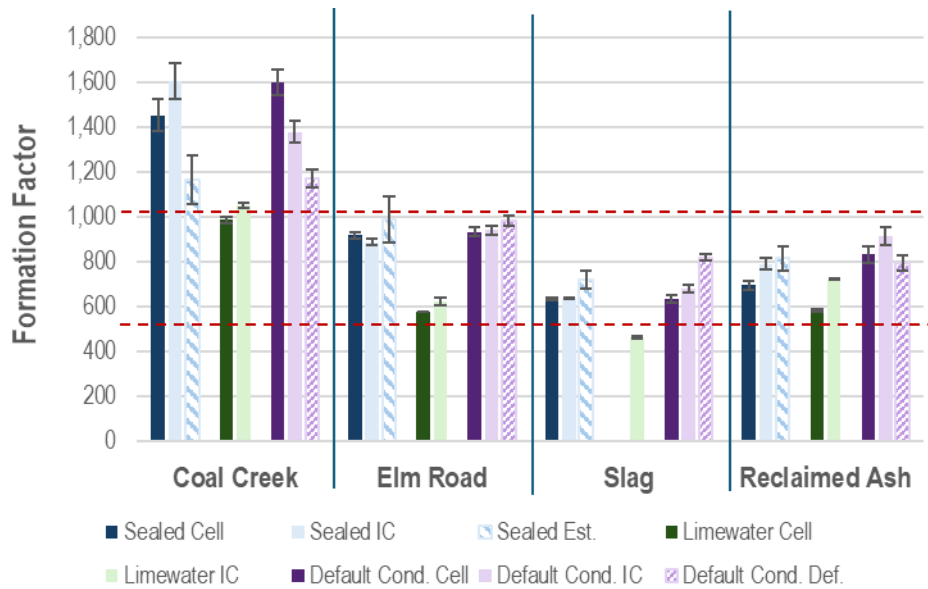


Figure 18 – Formation factor calculated using different means of obtaining pore solution resistivity. Cell indicates formation factor calculated using pore solution resistivity obtained using the pore solution cell, IC indicates that chemical composition was determined by ion chromatography and formation factor was calculated using pore solution resistivity obtained by the Snyder *et al.* [23] model, and Def, formation factor was calculated using the default value for the pore solution resistivity.

A one factor Analysis of Variance (ANOVA) test followed by a Tukey Honestly Significant Difference (HSD) with a 95% confidence was performed.

With the exception of Reclaimed Ash, the FF calculated using the experimentally obtained pore solution resistivity was statistically different than that using the default value of 0.127 ohm-m. For

the Slag and Elm Road mixtures, the FF using the default value was higher than that obtained using experimental values, while for Coal Creek, it was the opposite. This is because for Coal Creek, the pore solution resistivity obtained experimentally was 0.093 ohm-m, compared to the default value of 0.127 ohm-m, and for the Slag the experimentally obtained pore solution resistivity was 0.164 ohm-m. In these cases, it is clear that the assumption that there is equilibrium between the pore solution and the conditioning solution is not valid, even after 90 days of conditioning. It is important to highlight that ASTM C1876 allows cores to be conditioned for as little as 6 days, which is expected to result in even bigger differences between the pore solution resistivity and the default conditioning solution resistivity, increasing the error of the FF. The inability to achieve equilibrium in the default conditioning solution was also observed in other studies [42], [43].

The statistical analysis showed that there was a significant difference in FF for different conditionings. In general, the DC yielded the highest FF and limewater the lowest.

As mentioned previously, FF is a fundamental property that provides information on the fluid-filled pore volume and how the fluid-filled pores are interconnected among each other, i.e., a measure of the microstructure of the concrete. Therefore, it is reasonable to expect that the FF to be about the same, independent of the type of conditioning. However, this is not what was observed. There was a statistical difference in FF among the conditionings. For all the mixtures, except for the Slag, the default conditioning resulted in the highest FF. The difference in FF, as a function of conditioning indicate that the conditioning itself affects the reaction kinetics, as seen with the results of the DOR and the reaction products, resulting in differences in microstructure, as shown by the results of the mercury intrusion porosimetry (section 7.2.4).

AASHTO R 101 requires a minimum FF of 500 for mixtures not exposed to freezing and thawing and 1,000 for mixtures exposed to freezing and thawing and deicers. Interestingly, despite the historical good performance in the field of mixtures containing Elm Road and Slag, neither of these mixtures nor the Reclaimed Ash mixture met the requirement for freeze-thaw exposure.

The Coal Creek mixture presented the highest formation factor when comparing each conditioning. This indicated that it possesses a denser microstructure than the other mixtures.

7.2.6. Service Life

The formation factor is related to the diffusion coefficient by the Nermst-Einstein relationship [57] (Equation 8):

$$FF = \frac{D_0}{D} \quad \text{Equation 8}$$

Where:

D_0 = self-diffusion coefficient, which describes how the ionic species move through water (Table 7).

D = concrete effective diffusion coefficient.

Table 8 presents the self-diffusion coefficients for some ionic species.

Table 8 – Self Diffusion Coefficient [58]

Ionic Species	Self-Diffusion Coefficient, $10^{-10} \text{ m}^2/\text{s}$		
	32 °F	64 °F	77 °F
OH ⁻	25.6	44.9	52.7
Cl ⁻	10.1	17.1	20.3
SO ₄ ²⁻	5.0	8.9	10.7

Hence, with the FF results, the diffusion coefficient for each of the mixtures and conditionings can be calculated using Equation 8 (Table 9). From Table 9, with the exception of Coal Creek, there was no significant difference between the diffusion coefficient of the default conditioning determined experimentally and that calculated using the default value. Furthermore, for all mixtures but the Coal Creek mixture, there was no significant difference in diffusion coefficient across all types of conditioning.

Table 9 – Calculated Effective Concrete Chloride Diffusion Coefficient.

Mixture	Effective Concrete Chloride Diffusion Coefficient m^2/s at 77 °F				
	Sealed _{cell} [*]	Sealed _{est.} [*]	Limewater ^{**}	Default Conditioning _{cell} ^{**}	Default Conditioning _{def} ^{**}
Coal Creek	7.35×10^{-13}	9.17×10^{-13}	1.08×10^{-12}	6.68×10^{-13}	9.12×10^{-13}
Elm Road	1.16×10^{-12}	1.08×10^{-12}	1.85×10^{-12}	1.14×10^{-12}	1.08×10^{-12}
Slag	1.68×10^{-12}	1.48×10^{-12}	***	1.68×10^{-12}	1.30×10^{-12}
Reclaimed Ash	1.53×10^{-12}	1.31×10^{-12}	1.83×10^{-12}	1.28×10^{-12}	1.35×10^{-12}
* At 56 days		** At 91 days		*** Not determined	

The error function solution to Fick’s second law (Equation 9) can then be used to determine the time to initiate corrosion, assuming $C(x,t)$ 0.05% by mass of concrete, C_0 as 0.02% by mass of concrete, cover as 2 in., C_s 0.1% and that effective chloride diffusion coefficient is equal to the apparent chloride diffusion coefficient.

$$\frac{C(x, t) - C_0}{C_s - C_0} = 1 - \text{erf} \left(\frac{x}{2\sqrt{Dt}} \right) \quad \text{Equation 9}$$

Where:

$C(x,t)$ = ionic concentration at a depth x at an exposure time t

C_0 = background chloride content

C_s = surface concentration, which depends on the level of chloride exposure

D = apparent chloride diffusion coefficient

x = depth

t = time

Table 10 shows the time of corrosion initiation. However, it appears that the calculated service life varies depending on the conditioning. For example, for Coal Creek, limewater would result in 46 years, while the default conditioning would result in 75 years, a difference of 29 years. More interestingly is that for the same default conditioning, if FF was calculated based on experimentally obtained value of the pore solution resistivity, the service life would be 19 years higher than if the FF was calculated based on the pore solution resistivity default value of 0.127 ohm-m. This exemplifies the inadequacy of using a default value for the pore solution resistivity.

Table 10 – Calculated Time for Corrosion Initiation.

Mixture	Corrosion Initiation, years				
	Sealed _{cell} *	Sealed _{est.} *	Limewater**	Default Conditioning _{cell} **	Default Conditioning _{def} **
Coal Creek	68	56	46	75	56
Elm Road	43	47	27	44	47
Slag	30	34	***	30	36
Reclaimed Ash	33	39	28	40	37

* At 56 days ** At 91 days *** Not determined

FF also relates to freeze-thaw durability, assuming that the aggregates are freeze-thaw durable. AASHTO R 101 defines that concrete is freeze-thaw durable as long as the saturation of the concrete is below the critical degree of saturation (DOS_{crit}) (Equation 10). The DOS_{crit} is assumed to be 85%.

$$S(t) = S_{nick} + S_2\sqrt{t} \leq DOS_{crit} \quad \text{Equation 10}$$

Where:

S(t) = saturation as a function of time

S_{nick} = degree of saturation for a concrete where the gel and capillary pores are filled.

t = time

S_2 = a parameter related to the rate of saturation (Equation 11)

$$S_2 = 0.581 \sqrt{\frac{1}{FF} + 0.021} \quad \text{Equation 11}$$

Table 11 shows the calculated S_2 based on the FF for each mixture and conditioning type.

Table 11 – Calculated S_2 .

Mixture	S_2				
	Sealed _{cell} *	Sealed _{est.} *	Limewater**	Default Conditioning _{cell} **	Default Conditioning _{cell} **
Coal Creek	0.0362	0.0380	0.0395	0.0355	0.0380
Elm Road	0.0402	0.0395	0.0452	0.0400	0.0395
Slag	0.0440	0.0426	***	0.0440	0.0413
Reclaimed Ash	0.0430	0.0413	0.0450	0.0411	0.0416
* At 56 days		** At 91 days		*** Not determined	

In order to determine the effect of conditioning on the calculated time to reach the DOS_{crit} , the following ratio was calculated (Equation 12):

$$R_t = \frac{t_n}{t_{DCdef}} \quad \text{Equation 12}$$

Where:

t_n = calculated time to reach DOS_{crit} for each conditioning type

t_{DCdef} = calculated time to reach DOS_{crit} for default conditioning, using the default value for the pore solution resistivity (0.127 ohm-m).

Table 12 presents the ratio R. Assuming that the S_{nick} is the same for all conditionings, as can be seen, the time to achieve critical saturation is different depending on the conditioning type. For example, for Coal Creek, the calculated time to reach DOS_{crit} in the default conditioning using the pore solution resistivity obtained experimentally is 14% higher than that for the same conditioning but using the default value for pore solution resistivity. On the other hand, for Elm Road, this difference in time is only 2% lower. This shows that the error in calculating FF using a default value for the pore solution resistivity to infer freeze-thaw durability will depend on the mixture, i.e., the higher the difference of the pore solution resistivity obtained experimentally and the default value of 0.127 ohm-m, the higher this error.

If the calculated time to reach DOS_{crit} for specimens cured in limewater is compared to the time for specimens in default conditioning (DC_{cell}), the time for limewater cured specimens would be up to 22% lower than those in the default conditioning. This is probably due to the effect of the conditioning on the microstructure, as shown in section 7.2.4.

For Reclaimed Ash mixture, there is not a single conditioning that outperforms or underperforms significantly the other conditionings.

For each specific conditioning, there was a significant difference among the different SCMs, indicating that bulk resistivity can be used to differentiate mixtures.

The bulk resistivity of the AC specimens was lower than those in limewater, yet this difference was less than 10%.

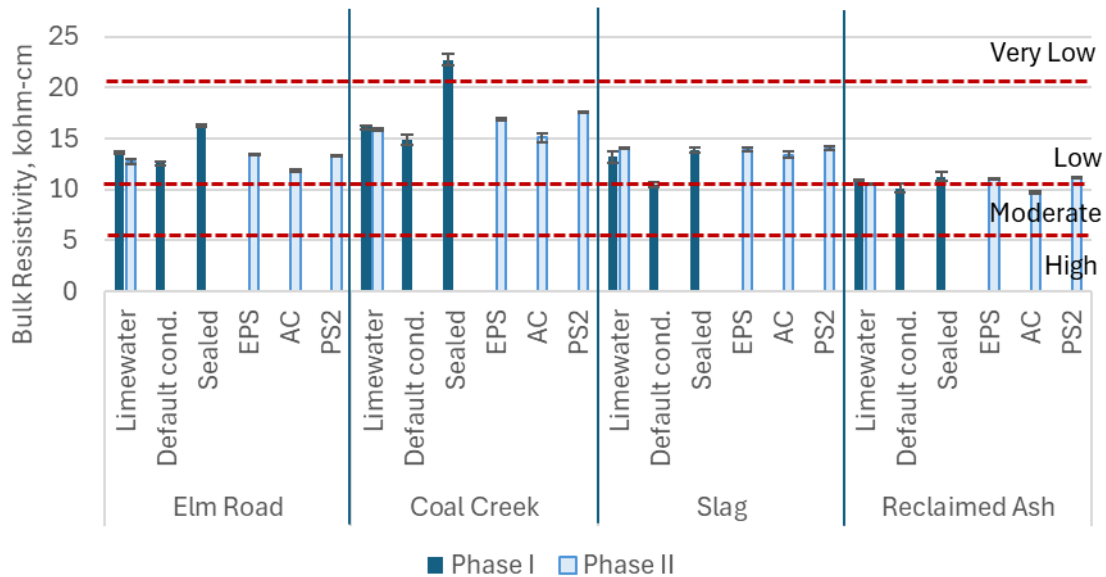


Figure 19 – Bulk resistivity of sealed specimens at 56 days. Bulk resistivity of AC at 28 days and all other conditionings at 91 days.

Figure 20 shows the effect of conditioning on the FF. The horizontal lines are thresholds from AASHTO R 101: for concrete not subjected to freezing and thawing $FF \geq 500$ and for concrete exposed to freezing and thawing and deicing salts $FF \geq 1000$.

For the Elm Road mixture, the default conditioning seemed to reach equilibrium since the FF obtained experimentally was similar to that using the default value of 0.127 ohm-cm. The same way, PS2 seemed to have reached equilibrium, since the FF calculated using experimental values was similar to that using the default value for the resistivity of the pore solution (0.152 ohm-cm). The FF for the default conditioning, sealed and EPS was similar. The pore solution resistivity estimated by the Montanari model showed good agreement with the value obtained experimentally, since the FF for sealed cell and sealed est. are similar. AC yielded the lowest FF that did not meet the minimum requirement of 500. One can hypothesize that the accelerated curing resulted in a much different microstructure than the other conditionings. None of the conditionings resulted in FF above the minimum requirement for freeze-thaw exposure.

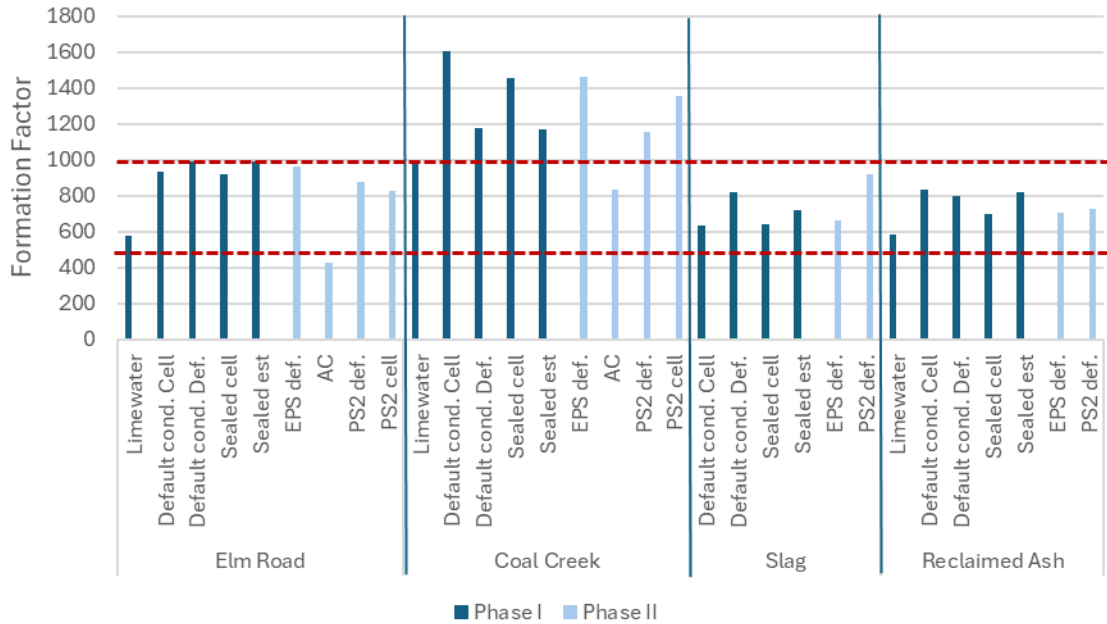


Figure 20 – Effect of conditioning on formation factor. Horizontal lines indicate requirements in AASHTO R 101. FF of AC at 28 days and all other conditionings at 91 days.

The Coal Creek mixture showed the largest spread of results among the conditionings, compared to the other mixtures. FF varied from 1602 to 836. For this mixture, no equilibrium was achieved in the default conditioning, since the FF obtained using experimental values was different than that using the default value for the pore solution. The same way, PS2 conditioning did not reach equilibrium either, showing that for this mixture, PS2 is not a good conditioning. The estimation for sealed was not similar to the FF obtained with experimental values. The sealed resulted in similar FF to the EPS. AC showed the lowest FF and did not meet the requirement for freeze-thaw exposure.

For the Slag mixture, the default conditioning did not reach equilibrium and the Montanari model provided good estimation. None of the conditionings passed the requirement for freeze-thaw exposure.

For the Reclaimed Ash mixture, the default conditioning reached equilibrium. None of the conditionings met the freeze-thaw exposure requirement.

The Coal Creek mixture presented the highest formation factor, indicating the denser microstructure comparing to the other mixtures.

7.3.2. Effect of the Coarse Aggregate

The Elm Road mixture prepared in Phase 1 was rebatched but two other coarse aggregates were used: Earl or Dresser Trap Rock. The conditionings used were limewater (LW) and default conditioning (DC). Figure 21 shows the effect of coarse aggregate on bulk resistivity at 91 days. For LW, all the bulk resistivity of the mixtures with the three different aggregates were statistically significant different, while for DC, the mixtures with Lannon and Dresser Trap were considered statistically the same.

Figure 21 shows that the aggregates affected bulk resistivity. However, independent of the aggregate and conditioning, with exception of Dresser in limewater, they were classified as low penetrability.

Figure 22 shows the effect of coarse aggregate on FF. FF calculated with the pore solution resistivity default value was higher than when the values obtained experimentally were used, especially for the Dresser mixture. FF showed to be dependent on the coarse aggregate type. This may be due to the aggregate morphology and the bond between the aggregate and the paste [59]. For the Lannon mixture, equilibrium between pore solution and conditioning solution was achieved, but not for the Dresser mixture. None of the FF calculated using experimental values achieved the minimum requirement for freeze-thaw exposure.

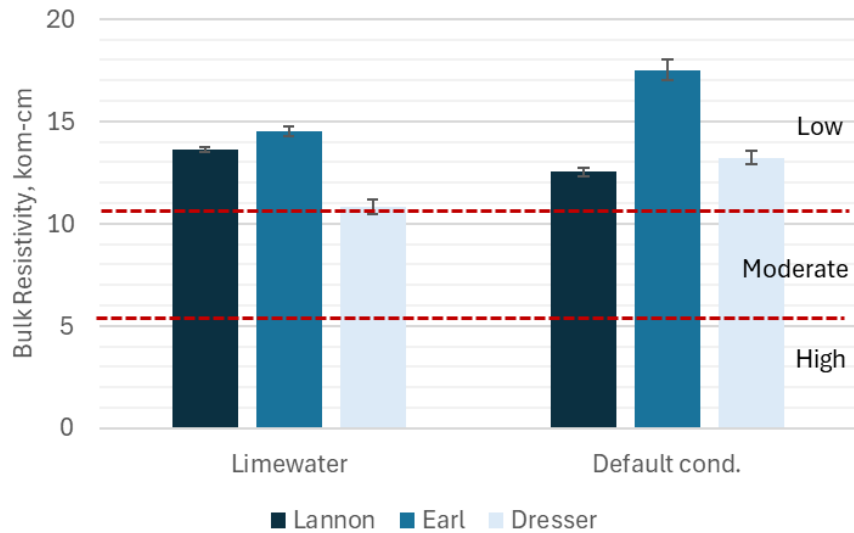


Figure 21 – Effect of coarse aggregate on bulk resistivity at 91 days.

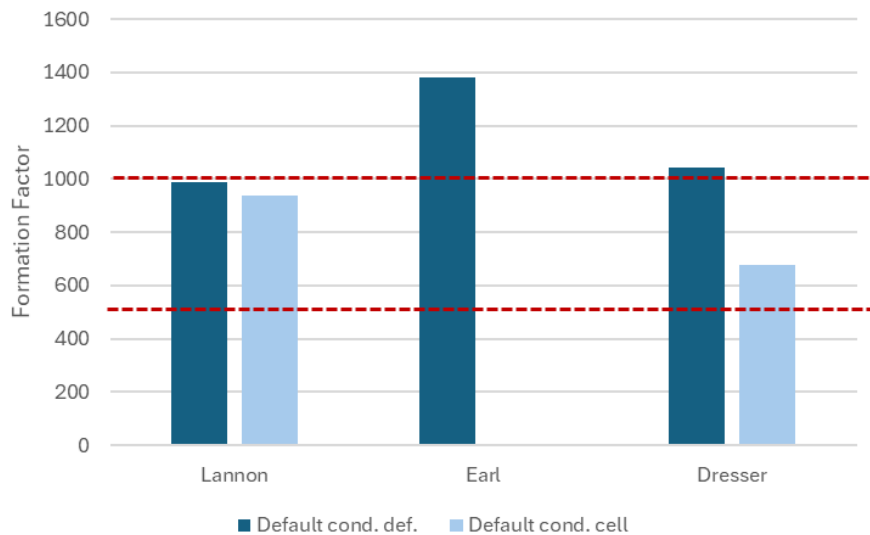


Figure 22 – Effect of coarse aggregate on formation factor at 91 days. Horizontal lines indicate requirements in AASHTO R 101.

7.3.3. Effect of the w/cm

The Coal Creek and the Elm Road mixtures prepared in Phase 1 were rebatched but the w/cm was reduced to 0.37. The conditionings used were limewater (LW), default conditioning (DC) and the estimated pore solution (EPS). Figure 23 shows the effect of w/cm on bulk resistivity at 91 days.

For both Coal Creek and Elm Road mixtures, the bulk resistivity of each conditioning was statistically different than the others. In addition, the bulk resistivity of the mixture with w/cm of 0.37 was higher than that of the mixture with w/cm of 0.45, for each of the conditionings, as expected. The lower w/cm results in a denser microstructure which, in turn, leads to higher bulk resistivity. This indicates that bulk resistivity can be used to differentiate mixtures with different w/cm. All mixtures, independent of the conditionings, were classified as low penetrability.

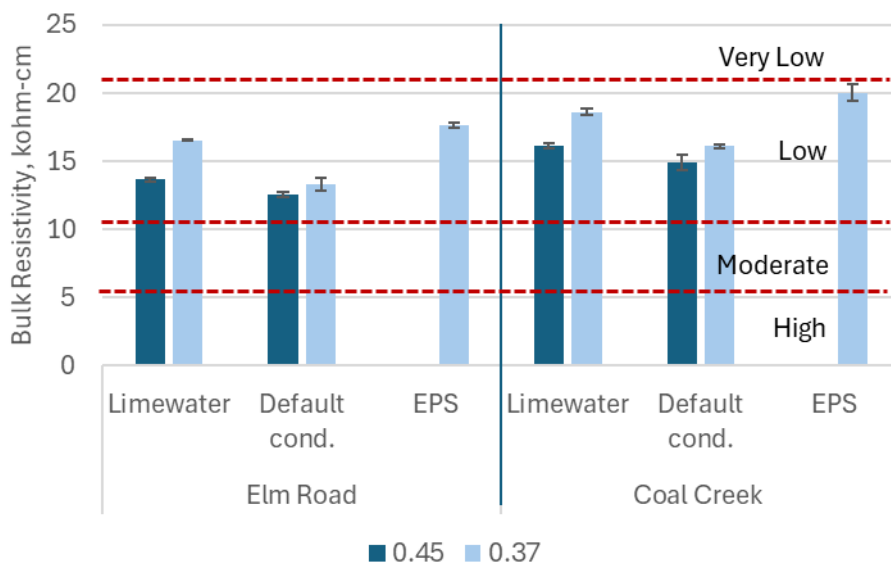


Figure 23 – Effect of w/cm on bulk resistivity.

Figure 24 shows the effect of w/cm on the FF. Surprisingly, the difference between the FF of the 0.37 mixture and the FF of the 0.45 mixture is not significant, although one can assume that the microstructure of the 0.37 mixture is much denser than that of the 0.45 mixture. The FF of the Elm Road mixture was 1043 for w/cm 0.37, compared with 935 of Phase I for w/cm of 0.45. The FF of Coal Creek mixture was 1269 for w/cm 0.37, compared to 1173 for w/cm 0.45. This may be an indication that FF is not properly reflecting the microstructure of the concrete.

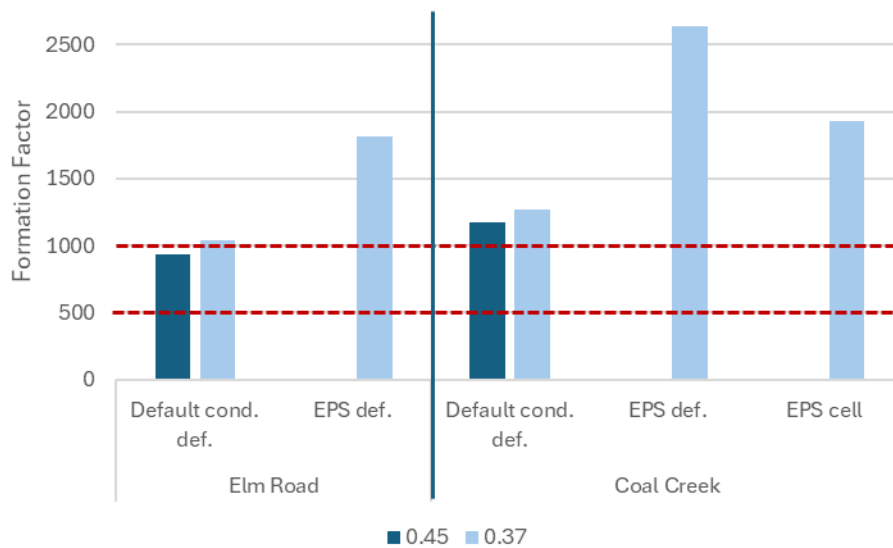


Figure 24 – Effect of w/cm on formation factor at 91 days. Horizontal lines indicate requirements in AASHTO R 101.

EPS conditioning presented a much higher FF than the default conditioning. EPS is a conditioning solution that is closer to the pore solution of the concrete than the default conditioning solution. This may represent the true FF of the concrete. The 0.37 mixtures met the minimum requirement for freeze-thaw exposure, independently of the conditioning.

7.3.4. Effect of the % of Cement Replacement

The Coal Creek, the Elm Road, and the Slag mixtures prepared in Phase 1 were rebatched but the cement replacement was decreased to 15%. The conditionings used were limewater (LW), default conditioning (DC) and the accelerated curing (AC). Figure 25 shows the effect of % cement replacement on bulk resistivity at 91 days.

It is clear that mixtures containing 30% of SCM resulted in significantly higher bulk resistivity, in comparison with those containing only 15%. This was expected, since SCMs densify the matrix, contributing to an increase in resistivity. This indicates that bulk resistivity can differentiate mixtures with different cement replacement levels, as long as there is a significant difference in these levels (Figure 25).

DC resulted in the lowest bulk resistivity. AC was 8 to 16% higher than LW, depending on the mixture and 2 to 28% higher than DC, also depending on the mixture.

The 15% SCM mixtures, independent of conditionings, were classified as moderate penetrability, while the 30% SCM, with exception of slag in default conditioning, were classified as low penetrability.

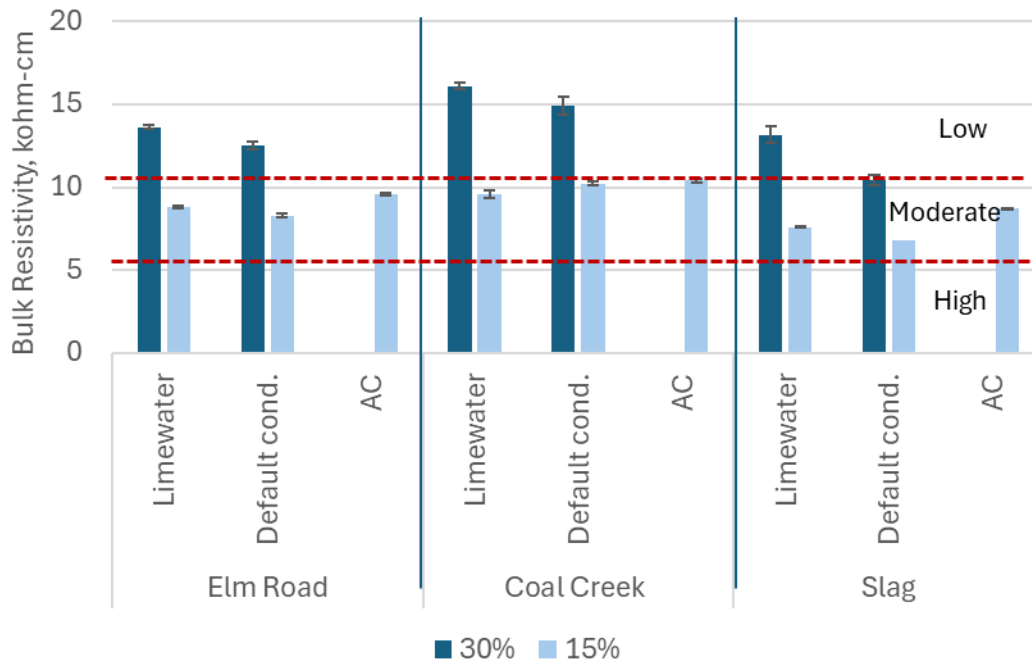


Figure 25 – Effect of % cement replacement on bulk resistivity.

Figure 26 shows the effect of % cement replacement on FF. As expected, the higher the percent cement replacement, the higher the FF. For the 30% Coal Creek mixture there was a significant difference between FF calculated with the default value for the resistivity of conditioning solution and the FF calculated based on experimental values. However, for the 15% Coal Creek mixture, this difference was small, indicating that the default conditioning solution may be appropriate to some mixtures but not all. For the 15% mixtures, as for the 30% mixtures, FF is dependent on the conditioning. AC presented the significantly lower FF and doesn't seem to be representative of the potential microstructure of the concrete in the field. AC resulted in FF that did not meet the minimum requirement of 500. None of the 15% SCM mixtures, independently of the conditioning, met the requirement for freeze-thaw exposure.

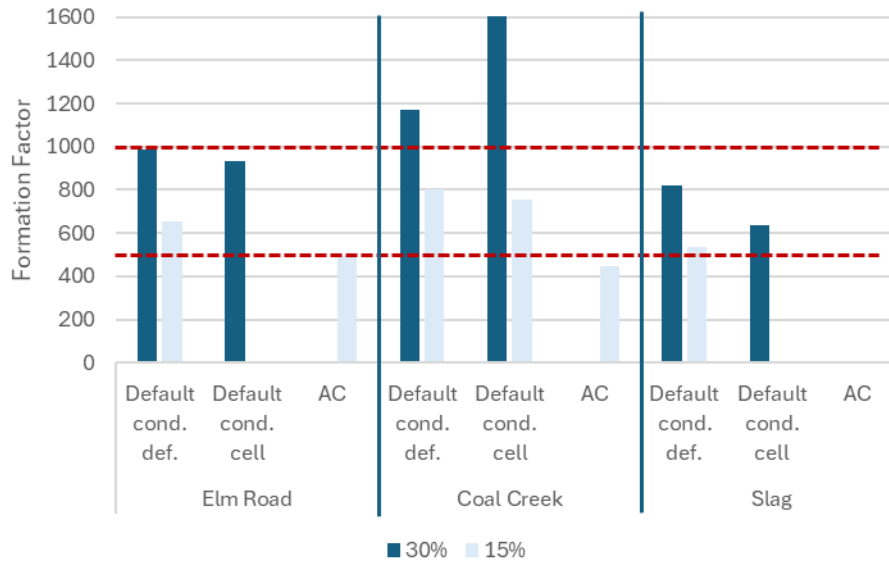


Figure 26 – Effect of % cement replacement on formation factor. AC at 28 days and DC at 91 days. Horizontal lines indicate requirements in AASHTO R 101.

7.3.5. Effect of Cement

The mixtures prepared in Phase I were rebatched using Continental Type IL cement. The conditionings used were limewater (LW), default conditioning (DC) and sealed (SL). Figure 27 shows the effect of the cement on bulk resistivity at 91 days. Once more, the conditioning affected the bulk resistivity of the mixtures.

For DC and sealed conditionings, the mixtures containing Continental cement resulted in higher bulk resistivities. For LW, the Coal Creek mixture with Alpena cement resulted in higher resistivity than that with Continental cement, for the Elm Road mixture it was the exact opposite and for the Slag and Reclaimed Ash mixtures there was no significant difference between the mixtures with Alpena and Continental cements. Thus, bulk resistivity was not capable of differentiating mixtures with different cement of the same class (Type IL).

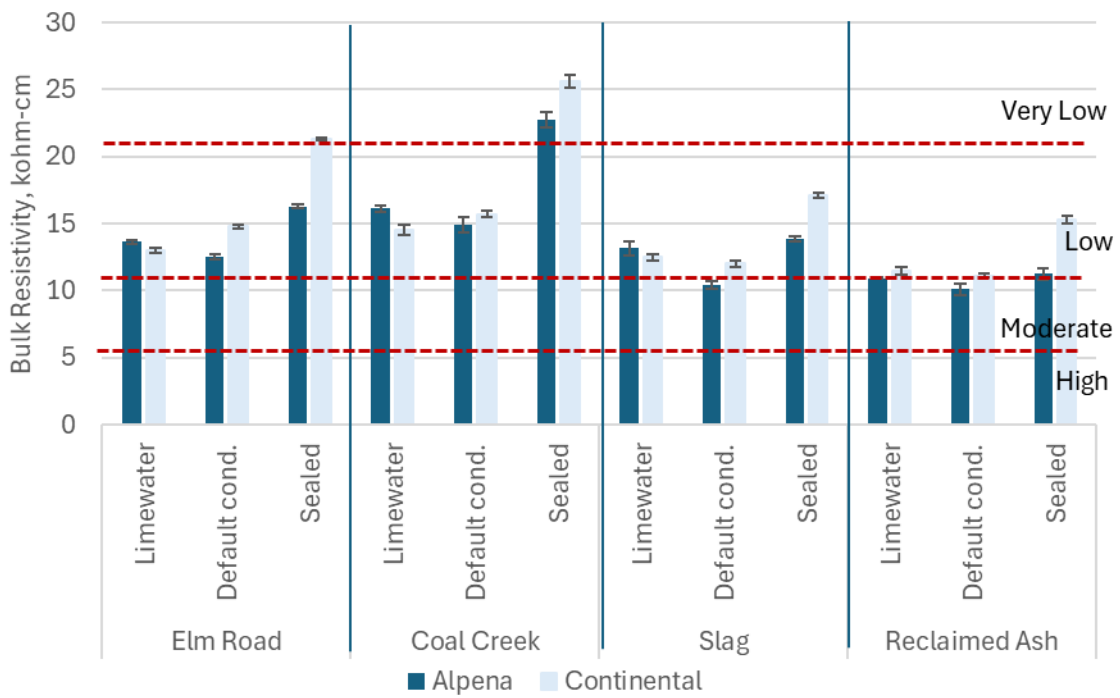


Figure 27 – Effect of cement on bulk resistivity. Sealed at 56 days, other conditionings at 91 days.

Figure 28 shows the same trend as the bulk resistivity, i.e., there was not a significant difference on the FF for the two cements used.

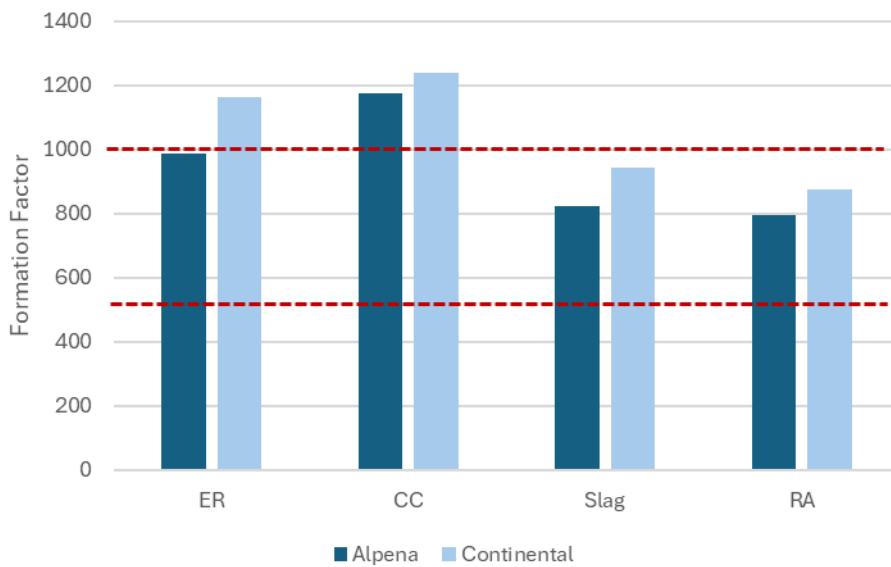


Figure 28 – Effect of cement on formation factor with default conditioning. Horizontal lines indicate requirements in AASHTO R 101.

7.3.6. Effect of Age

Figure 29 shows the increase in bulk resistivity from 56 to 91 days. Although there is limited data, it is clear that the bulk resistivity of slag mixtures and mixtures in LW increased less from 56 to 91 days than all the other sets in this study. The average increase for slag mixtures was 22% and 23% for mixtures in LW, while for all the other sets, the increase in bulk resistivity between 56 and 91 days was, in average, 44%. This shows that the conditioning may be affecting the hydration of the cementitious materials.

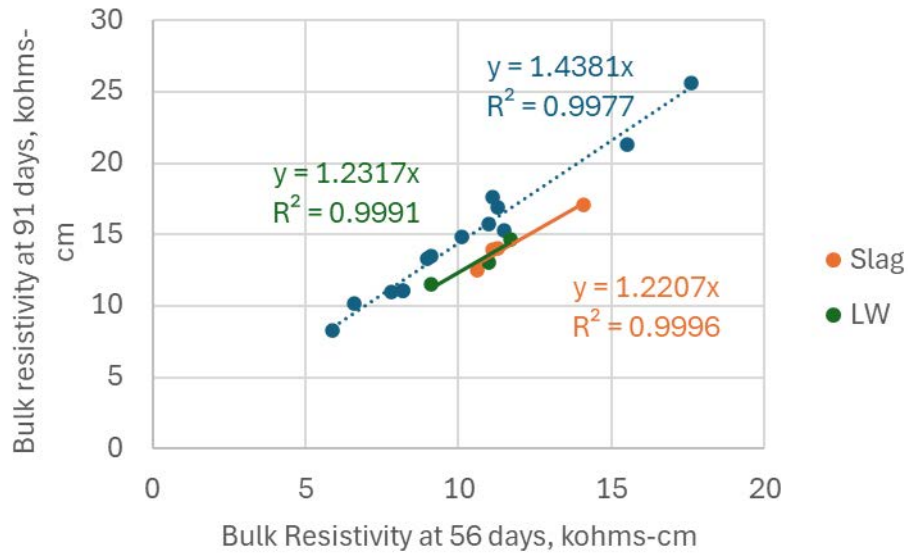


Figure 29 – Effect of age on bulk resistivity.

7.3.7. Relationship between Surface Resistivity and Bulk resistivity

Figure 30 shows a good correlation between surface and bulk resistivities. Figure 30a shows the data per type of conditioning. As can be seen, most of the data is within $\pm 10\%$. The correlation between surface and bulk resistivities is about 1, with exception of the mixtures conditioned in DC.

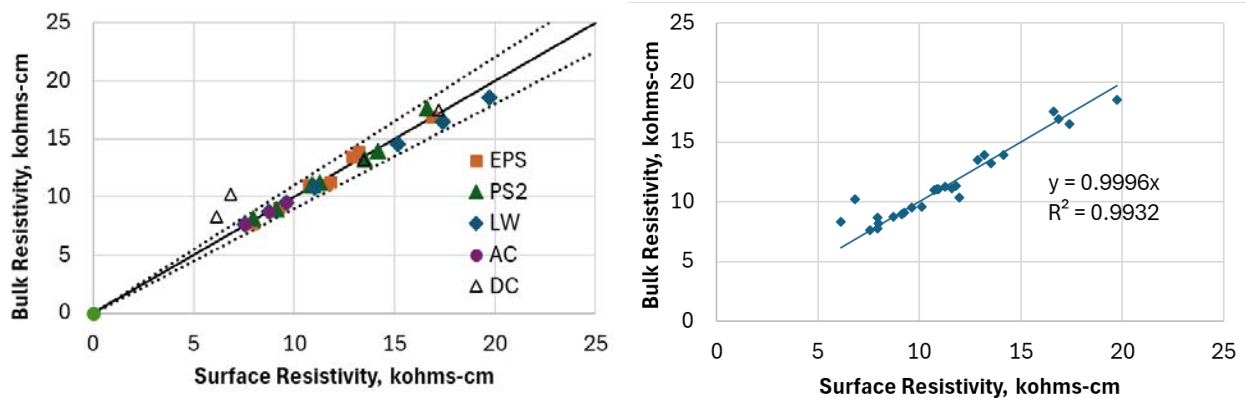


Figure 30 – Correlation between surface resistivity and bulk resistivity. (a) by conditioning type, (b) all data. Dashed line indicates $\pm 10\%$.

7.3.8. Relationship between Bulk Resistivity and RCPT

Figure 31 shows that the correlation between bulk resistivity and RCPT was not as good as expected. If one considers the penetrability classification in the RCPT and applies the classification in WTM T358[54] to the bulk resistivity results, out of the 24 data set point, there are 5 mismatch classifications. In 4 of them, bulk resistivity provides a more conservative classification than the RCPT.

As shown in Figure 1, different curves correlating RCPT and resistivity have been proposed over the years. As a result, different boundaries for the penetrability classification can be obtained, depending on the curve used. The reason for the curves to be different can be the mixture proportions of the concretes used to develop the curves, and the volume ratio between limewater and concrete. Table 13 shows two penetrability classifications based on two different curves and what would be the classification based on the curve shown in Figure 31. Since the curve in Figure 31 did not match the curve used to develop the classification in WTM T358, there is a mismatch in classification. Another reason for mismatch between the curve in Figure 31 and the one used to develop the WTM T358 is that in Figure 31, different conditionings were used, not only limewater.

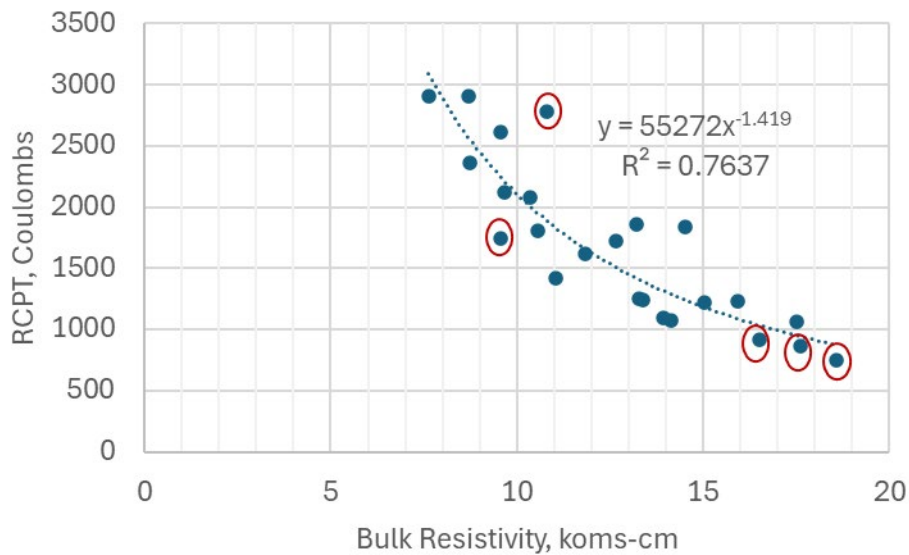


Figure 31 – Correlation between bulk resistivity and RCPT. Circled points indicate mismatch in classification between resistivity and RCPT.

Table 13 – Chloride Penetrability Classifications.

	WTM T358*	T 358**	Based on Figure 31
High	<5.2	<6.2	<6.4
Moderate	5.2-10.4	6.2-10.9	6.4-10.4
Low	10.4-20.8	10.9-19.2	10.4-16.9
Very Low	20.8-207	19.2-132	16.9-86

Negligible	>207	>132	>86
* These boundaries were obtained by correlating RCPT and bulk resistivity.			
** Values converted from apparent surface resistivity to surface resistivity. These boundaries were obtained by correlating RCPT and apparent surface resistivity.			

8. CONCLUSIONS AND RECOMMENDATIONS

An extensive experimental program was carried out. The effect of different conditionings on bulk resistivity, formation factor, microstructure and service life was evaluated. The effect of materials and mixture proportions on bulk resistivity and formation factor was also assessed.

The types of conditioning evaluated were limewater, sealed, ASTM C1876 default conditioning, an average pore solution for WisDOT mixtures, an estimated pore solution of each mixture, and accelerated curing.

Bulk resistivity was affected by the aggregate, percentage of SCM, w/cm, cement and conditioning.

Formation factor was affected by the aggregate, percentage of SCM, w/cm and conditioning.

Formation factor is an intrinsic material property that reflects its microstructure. However, it was observed that formation factor was a function of the conditioning. This is because the conditioning method may affect the reactions kinetics, the porosity and the pore size, and, consequently the bulk resistivity and the formation factor.

The most accurate conditioning solution for the determination of formation factor was found to be the one that requires the solution to be estimated for every single mixture (EPS). Nevertheless, this process is cumbersome and may yield errors in solution preparation when many different mixtures need to be evaluated. The average pore solution (PS2) was found to be more accurate than the default conditioning. For the default conditioning, the equilibrium between the pore solution and the conditioning solution is not always achieved, even after 90 days of conditioning, resulting in inaccurate formation factors. Moreover, conditioning specimens in solutions requires large solution volumes, is expensive, and requires proper handling and disposal.

The accelerated curing can be used for bulk resistivity and shouldn't be used for formation factor.

The modified NIST model (Montanari model) provided a good estimation of the resistivity of the pore solution and can be used to determine the formation factor.

Service life and time to reach critical saturation were estimated. They were a function of the conditioning method, since they are a function of the formation factor.

8.1. Recommendations

It is recommended that formation factor be used for mixture qualification.

AASHTO R 101 requirement for freeze-thaw exposure ($FF \geq 1,000$) was found to be too restrictive. Mixtures that perform well in the field did not meet this requirement. Based on limited data from this project, a FF greater than or equal to 700 seems to be a more reasonable limit.

However, more research is needed correlating the formation factor and the freeze-thaw performance.

The most practical method to determine formation factor is to use the sealed condition, as long as the specimens are properly sealed. This conditioning may be more representative of the concrete in the field, except during rain season or snow thawing, and allows the pore solution resistivity to be estimated. Sealing specimens is more easily implementable than conditioning in a solution, since it doesn't require three specimens to be conditioned in each bucket, reducing the laboratory space needed, and doesn't require the preparation or disposal of any solution. It is recommended specimens to be kept in their molds with lids, tape the area between lid and mold and double-bag the specimens in plastic bags, properly closed. The specimens should be then kept in a moist room until age of testing.

At the age of 91 days, the specimens are demolded and the resistivity determined. The resistivity of the pore solution is determined by the Montanari model and the formation factor is calculated (Figure 32). For the Montanari model, 90% can be used the degree of reaction at 91 days.

During the qualification process, a correlation between the resistivity of the sealed specimens and the resistivity of the limewater or accelerated curing specimens are obtained.

For quality control/quality assurance, instead of using formation factor, the resistivity of limewater or accelerated curing specimens can be used, using the values obtained during mixture qualification as thresholds (Figure 32).

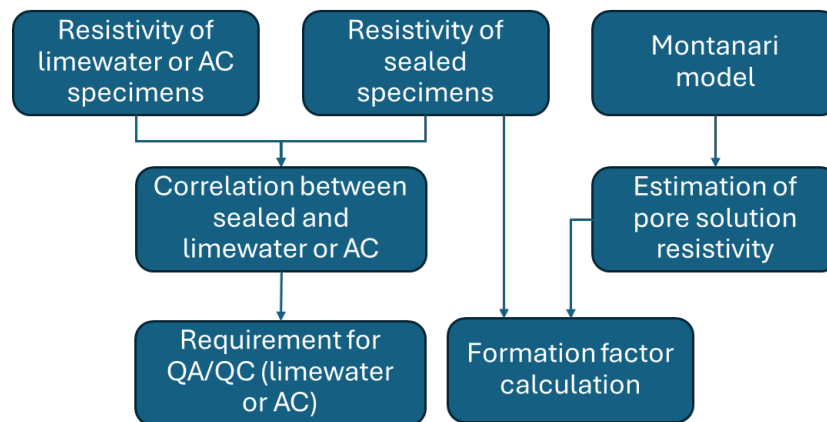


Figure 32 – Recommendation for implementation of formation factor for mixture qualification and resistivity for QA/QC.

ASTM C1876 allows cores to be conditioned for a minimum of 6 days. In this project, it was found that, in some cases, 90 days of conditioning in the default conditioning was not sufficient to reach the equilibrium between the pore solution and the conditioning solution. The further away from the equilibrium that it is, the higher the error in calculating formation factor. So, it is not recommended for the cores to be conditioned for only 6 days. More research is needed to determine the minimum conditioning time.

8.1.1. Recommended Specification Language

During the qualification process, at 91 days, determine the resistivity of sealed specimens and companion specimens cured in limewater or subjected to accelerated curing. Sealed specimens shall be kept in the molds, the area between the lid and the mold shall be taped and the specimens placed in double plastic bags, properly closed. Then, the specimens shall be placed in a moist room until the age of 91 days. Specimens subjected to accelerated curing shall be cured in saturated limewater at 73 ± 3 °F for 7 days. Then, specimens shall be cured at 100 ± 3 °F until the age of 28 days. A correlation between the formation factor of sealed specimens and the resistivity of limewater specimens or accelerated cured specimens shall be established and this value shall be used for QA/QC.

To determine the formation factor, input the values of the cement and SCM chemical composition in the provided spreadsheet for pore solution modeling and determine the pore solution resistivity. Calculate the formation factor by dividing the resistivity of the sealed specimens by the calculated resistivity of the pore solution. Formation factor shall be equal to or higher than 500, if the concrete will not be exposed to freezing and thawing and deicing salts. For concretes exposed to freezing and thawing and deicing salts, the formation factor shall be equal to or higher than 700.

9. REFERENCES

- [1] J. Tanesi, L. Montanari, and A. Ardani, "Formation Factor Demystified and Its Relationship to Durability," *FHWA-HRT-19-030*, p. 10, 2019.
- [2] P. J. Tumidajski, A. S. Schumacher, S. Perron, P. Gu, and J. J. Beaudoin, "On the relationship between porosity and electrical resistivity in cementitious systems," *Cem. Concr. Res.*, vol. 26, no. 4, pp. 539–544, 1996, doi: 10.1016/0008-8846(96)00017-8.
- [3] W. Jason Weiss, R. P. Spragg, O. Burkan Isgor, M. Tyler Ley, and T. Van Dam, "Toward performance specifications for concrete: Linking resistivity, RCPT and diffusion predictions using the formation factor for use in specifications," in *High Tech Concrete: Where Technology and Engineering Meet - Proceedings of the 2017 fib Symposium*, 2017. doi: 10.1007/978-3-319-59471-2_235.
- [4] C. Qiao, A. T. Coyle, O. B. Isgor, and W. J. Weiss, "Prediction of Chloride Ingress in Saturated Concrete Using Formation Factor and Chloride Binding Isotherm," *Adv. Civ. Eng. Mater.*, vol. 7, no. 1, p. 20170141, 2018, doi: 10.1520/acem20170141.
- [5] FDOT, "Florida method of test for concrete resistivity as an electrical indicator of its permeability," 2004.
- [6] T. D. Rupnow and P. Icenogle, "Evaluation of Surface Resistivity Measurements as an Alternative to the Rapid Chloride Permeability Test for Quality Assurance and Acceptance July 2011 LTRC Project Number: 10-1C SIO Number: 30000111 Louisiana Transportation Research Center 4101 Gourrie," no. 2, pp. 100–101, 2011.
- [7] O. Sengul and O. E. Gjrv, "Electrical resistivity measurements for quality control during concrete construction," *ACI Mater. J.*, vol. 105, no. 6, pp. 541–547, 2008, doi: 10.14359/20195.
- [8] ASTM C1202-25, "Test Method for Electrical Indication of Concretes Ability to Resist Chloride Ion Penetration." ASTM International, West Conshohocken, PA, Jan. 01, 2025.

- doi: 10.1520/C1202-25.
- [9] A. R. Chini, L. C. Muszynski, and J. Hicks, "Determination of Acceptance Permeability Characteristics for Performance-Related Specifications for Portland Cement Concrete," 2003.
- [10] J. Tanesi and A. Ardani, "Surface Resistivity Test Evaluation as an Indicator of the Chloride Permeability of Concrete," *FHWA-HRT-13-024*, p. 6, 2013.
- [11] M. A. Helsel, L. Montanari, R. Spragg, I. de la Varga, and N. Saladi, "Correlating Durability Indicators to Resistivity and Formation Factor of Concrete Materials," *Transp. Res. Rec. J. Transp. Res. Board*, vol. 2677, no. 7, pp. 488–499, Jul. 2023, doi: 10.1177/03611981231153651.
- [12] R. Spragg *et al.*, "Leaching of conductive species: Implications to measurements of electrical resistivity," *Cem. Concr. Compos.*, vol. 79, pp. 94–105, 2017, doi: 10.1016/j.cemconcomp.2017.02.003.
- [13] F. Rajabipour, "In situ Electrical Sensing and Material Health Monitoring in Concrete Structures," Purdue University, 2006.
- [14] J. Weiss, K. Snyder, J. Bullard, and D. Bentz, "Using a Saturation Function to Interpret the Electrical Properties of Partially Saturated Concrete," *J. Mater. Civ. Eng.*, vol. 25, no. 8, pp. 1097–1106, 2012, doi: 10.1061/(ASCE)MT.1943-5533.0000549.
- [15] R. P. Spragg, I. De la Varga, L. Montanari, and B. Graybeal, "Using formation factor to define the durability of UHPC," in *Proceedings. 2nd International Interactive Symposium on UHPC*, Albany, NY, USA, 2019.
- [16] J. Tanesi, L. Montanari, and A. Ardani, "Formation Factor Demystified and its Relationship to Durability." FHWA, McLean, VA, 2019. doi: FHWA-HRT-19-044.
- [17] R. Spragg, C. Villani, and J. Weiss, "Electrical Properties of Cementitious Systems: Formation Factor Determination and the Influence of Conditioning Procedures," *Adv. Civ. Eng. Mater.*, vol. 5, no. 1, p. 20150035, Mar. 2016, doi: 10.1520/ACEM20150035.
- [18] R. Spragg, C. Qiao, T. Barrett, and J. Weiss, "Assessing a concrete's resistance to chloride ion ingress using the formation factor," *Corros. Steel Concr. Struct.*, pp. 211–238, 2016, doi: 10.1016/B978-1-78242-381-2.00011-0.
- [19] AASHTO R 101-22, "Standard Practice for Developing Performance Engineered Concrete Pavement Mixtures." 2022.
- [20] AASHTO PP 84-20(2021), "Standard Practice for Developing Performance Engineered Concrete Pavement Mixtures," vol. 1, no. April. American Association of State Highway and Transportation Officials, Washington, D.C., pp. 1–36, 2020.
- [21] L. Montanari, J. Tanesi, H. Kim, and A. Ardani, "Influence of Loading Pressure and Sample Preparation on Ionic Concentration and Resistivity of Pore Solution Expressed from Concrete Samples," *J. Test. Eval.*, vol. 49, no. 5, p. 20190765, Sep. 2021, doi: 10.1520/JTE20190765.
- [22] D. P. Bentz, "A virtual rapid chloride permeability test," *Cem. Concr. Compos.*, vol. 29, no. 10, pp. 723–731, 2007, doi: 10.1016/j.cemconcomp.2007.06.006.
- [23] K. . Snyder, X. Feng, B. . Keen, and T. . Mason, "Estimating the electrical conductivity of cement paste pore solutions from OH⁻, K⁺ and Na⁺ concentrations," *Cem. Concr. Res.*, vol. 33, no. 6, pp. 793–798, Jun. 2003, doi: 10.1016/S0008-8846(02)01068-2.

- [24] S. Diamond, “Effects of two Danish flyashes on alkali contents of pore solutions of cement-flyash pastes,” *Cem. Concr. Res.*, vol. 11, no. 3, pp. 383–394, 1981, doi: 10.1016/0008-8846(81)90110-1.
- [25] C. L. Page and Vennesland, “Pore solution composition and chloride binding capacity of silica-fume cement pastes,” *Matériaux Constr.*, vol. 16, no. 1, pp. 19–25, 1983, doi: 10.1007/BF02474863.
- [26] H. J. H. Brouwers and R. J. van Eijk, “Alkali concentrations of pore solution in hydrating OPC,” *Cem. Concr. Res.*, vol. 33, no. 2, pp. 191–196, 2003, doi: 10.1016/S0008-8846(02)01022-0.
- [27] B. Lothenbach, G. La Saout, E. Gallucci, and K. Scrivener, “Influence of Limestone on the Hydration of Portland Cement,” *Cem. Concr. Res.*, vol. 38, no. 6, pp. 848–860, 2008.
- [28] M. A. Bérubé, C. Tremblay, B. Fournier, M. D. Thomas, and D. B. Stokes, “Influence of lithium-based products proposed for counteracting ASR on the chemistry of pore solution and cement hydrates,” *Cem. Concr. Res.*, vol. 34, no. 9, pp. 1645–1660, 2004, doi: 10.1016/j.cemconres.2004.03.025.
- [29] B. Lothenbach and F. Winnefeld, “Thermodynamic modelling of the hydration of Portland cement,” *Cem. Concr. Res.*, vol. 36, no. 2, pp. 209–226, Feb. 2006, doi: 10.1016/j.cemconres.2005.03.001.
- [30] E. Schäfer, “Einfluss der Reaktionen des Zementbestandteile auf den alkali haushalt der Porelösung des Zementsteins,” 2004.
- [31] J. A. Larbi, A. L. A. Fraay, and J. M. J. M. Bijen, “The chemistry of the pore fluid of silica fume-blended cement systems,” *Cem. Concr. Res.*, vol. 20, no. 4, pp. 506–516, 1990, doi: 10.1016/0008-8846(90)90095-F.
- [32] F. Rajabipour, G. Sant, and J. Weiss, “Interactions between shrinkage reducing admixtures (SRA) and cement paste’s pore solution,” *Cem. Concr. Res.*, vol. 38, no. 5, pp. 606–615, May 2008, doi: 10.1016/j.cemconres.2007.12.005.
- [33] P. Longuet, “Protection des armatures dans le betone arme elabore avec des ciments de laitier,” *Silic In*, vol. 41, no. 7/8, 1976.
- [34] M. Nokken, “Development of Discontinuous Capillary Porosity in Concrete and its Influence on Durability,” 2004.
- [35] T. Chappex and K. Scrivener, “Controlling Alkali silica reaction by understanding alkali immobilization in C-S-H by SCMs,” *13th Int. Congr. Chem. Cem.*, 2011.
- [36] A. Vollpracht and W. Brameshuber, “Investigations on ten years old hardened cement paste samples,” *Int. Rilem Conf. Mater. Sci.*, 2010.
- [37] K. De Weerdt, M. Ben Haha, G. Le Saout, K. O. Kjellsen, H. Justnes, and B. Lothenbach, “Hydration mechanisms of ternary Portland cements containing limestone powder and fly ash,” *Cem. Concr. Res.*, vol. 41, no. 3, pp. 279–291, 2011, doi: 10.1016/j.cemconres.2010.11.014.
- [38] F. Deschner, B. Lothenbach, F. Winnefeld, and J. Neubauer, “Effect of temperature on the hydration of Portland cement blended with siliceous fly ash,” *Cem. Concr. Res.*, vol. 52, pp. 169–181, 2013, doi: 10.1016/j.cemconres.2013.07.006.
- [39] M. Tsui-Chang, P. Suraneni, L. Montanari, J. F. Muñoz, and W. Jason Weiss, “Determination of chemical composition and electrical resistivity of expressed cementitious

- pore solutions using X-ray fluorescence,” *ACI Mater. J.*, vol. 116, no. 1, pp. 155–164, 2019, doi: 10.14359/51712242.
- [40] L. J. Parrot and D. C. Killoh, “Prediction of cement hydration,” *Br Ceram Proc*, vol. 35, pp. 41–53, 1984.
- [41] K. De Weerd, G. Plusquellec, A. Belda Revert, M. R. Geiker, and B. Lothenbach, “Effect of carbonation on the pore solution of mortar,” *Cem. Concr. Res.*, vol. 118, pp. 38–56, Apr. 2019, doi: 10.1016/j.cemconres.2019.02.004.
- [42] L. Montanari, J. Tanesi, P. Hosseini, E. Stewartson, and M. A. Helsel, “Concrete Formation Factor: Experimental and Modeling Methods,” in *Proceedings of the 13th International Conference on Concrete Pavements*, Minneapolis: International Society for Concrete Pavements, 2024.
- [43] C. Obla, Karthik H, Lobo, “Electrical Tests for Concrete Penetrability, Part 2,” *ACI Mater. J.*, vol. 118, no. 5, Sep. 2021, doi: 10.14359/51732935.
- [44] ASTM C1876-24, “Test Method for Bulk Electrical Resistivity or Bulk Conductivity of Concrete.” ASTM International, West Conshohocken, PA, Jan. 01, 2024. doi: 10.1520/C1876-24.
- [45] AASHTO TP 119-22, “Standard Method of Test for Electrical Resistivity of a Concrete Cylinder Tested in a Uniaxial Resistance Test.” American Association of State Highway and Transportation Officials, Washington, D.C.
- [46] AASHTO T 119M/119-23, “Standard Method of Test for Slump of Hydraulic Cement Concrete.” American Association of State Highway and Transportation Officials, Washington, D.C., 2023.
- [47] AASHTO T 121M/T 121-23, “Standard Method of Test for Density (Unit Weight), Yield, and Air Content (Gravimetric) of Concrete.” American Association of State Highway and Transportation Officials, Washington, D.C., 2023.
- [48] AASHTO T 395-22, “Standard Method of Characterization of the Air-Void System of Freshly Mixed Concrete by the Sequential Pressure Method.” American Association of State Highway and Transportation Officers, 2022.
- [49] I. Pane and W. Hansen, “Investigation of blended cement hydration by isothermal calorimetry and thermal analysis,” *Cem. Concr. Res.*, vol. 35, no. 6, pp. 1155–1164, Jun. 2005, doi: 10.1016/j.cemconres.2004.10.027.
- [50] N. De Belie *et al.*, “Determination of the degree of reaction of fly ash in blended cement pastes,” in *14th International Congress on the Chemistry of Cement (ICCC2015)*, 2015, pp. 1–12.
- [51] W. Deboucha, N. Leklou, A. Khelidj, and M. N. Oudjit, “Hydration development of mineral additives blended cement using thermogravimetric analysis (TGA): Methodology of calculating the degree of hydration,” *Constr. Build. Mater.*, vol. 146, pp. 687–701, Aug. 2017, doi: 10.1016/j.conbuildmat.2017.04.132.
- [52] M. Meziani, N. Chelouah, O. Amiri, and N. Leklou, “Blended cement hydration assessment by thermogravimetric analysis and isothermal calorimetry,” *MATEC Web Conf.*, vol. 149, p. 01062, Feb. 2018, doi: 10.1051/mateconf/201814901062.
- [53] AASHTO T 22M/T22-22, “Standard Method of Test for Compressive Strength of Cylindrical Concrete Specimens.” American Association of State Highway and

- Transportation Officials, Washington, D.C., 2022.
- [54] Wisconsin Department of Transportation, “WTM T358, Manual of Test Procedures.” Wisconsin Department of Transportation, Bureau of Project Development, Madison, p. 168, 2024.
- [55] R. Spragg, Y. Bu, K. Snyder, D. Bentz, and J. Weiss, “Electrical Testing of Cement-Based Materials: Role of Testing Techniques, Sample Conditioning,” American Association of State Highway and Transportation Officials, Washington, D.C., Dec. 2013. [Online]. Available: <http://docs.lib.purdue.edu/jtrp/1544/>
- [56] L. Montanari, J. Tanesi, K. H. Obla, and C. L. Lobo, “Effect of Concrete Curing Conditions and Air Content on the Formation Factor and the Transport Properties Classifications Based on AASHTO PP84,” in *Proceedings of the 99th TRB Annual Meeting*, Washington, D.C., 2020.
- [57] K. A. Snyder, “The relationship between the formation factor and the diffusion coefficient of porous materials saturated with concentrated electrolytes: theoretical and experimental considerations.,” 2000.
- [58] L. Yuan-Hui and S. Gregory, “Diffusion of ions in sea water and in deep-sea sediments,” *Geochim. Cosmochim. Acta*, vol. 38, no. 5, pp. 703–714, May 1974, doi: 10.1016/0016-7037(74)90145-8.
- [59] D. P. Bentz *et al.*, “Influence of aggregate characteristics on concrete performance,” Gaithersburg, MD, May 2017. doi: 10.6028/NIST.TN.1963.

APPENDIX A

NIST Model

This model estimates the pore solution concentration of Na^+ , K^+ , and OH^- in a mixture and uses an electrochemical model [1] to determine the pore solution electrical resistivity from these estimated ionic concentrations. In this model, information on the mixture design, the cementitious material's chemical composition, and the degree of reaction.

Equation 1 and Equation 2 describe the mass fraction of the cementitious system which dissolves in solution, which is given by the sum of the contribution of the single cementitious material "i", multiplied by their respective free alkali ion factors.

Equation 3 and Equation 4 transform the sodium oxide and the potassium oxide which dissolved in solution from mass fraction to moles of sodium and potassium per g of material.

The final step for the ionic concentration calculation of sodium and potassium requires to normalize the moles of dissolved alkalis by the amount of free water in the pores per g of cementitious material (L/g) as described in Equation 5 and Equation 6. Equation 5 and Equation 6 take into account the dilution effect when a SCM is used.

Equation 7a represents the simplified case of a pure hydraulic system, where the free water is obtained by subtracting from the initial w/c the water that is bound in the hydration products, for which the value of 0.23 (ml/g) is commonly accepted. The presence of SCMs could be incorporated in the equation by adjusting the bound water value, proportionally to the mass replacement and the type of SCM (Equation 7b).

$$\text{Na}_2\text{O}(\text{Diss.}) = \sum_i^n \left(m_{f,i}^{(\text{Na}_2\text{O})} \cdot \frac{M_i}{M_{cm}} \cdot f_i \cdot 0.75 \right) \quad \text{Equation 1}$$

$$\text{K}_2\text{O}(\text{Diss.}) = \sum_i^n \left(m_{f,i}^{(\text{K}_2\text{O})} \cdot \frac{M_i}{M_{cm}} \cdot f_i \cdot 0.75 \right) \quad \text{Equation 2}$$

$$\text{Na}^+ \left(\frac{\text{mol}}{\text{g}} \right) = \frac{\text{Na}_2\text{O}(\text{Diss.}) \cdot 2}{(2 \cdot 22.9898 + 15.9994)} \quad \text{Equation 3}$$

$$\text{K}^+ \left(\frac{\text{mol}}{\text{g}} \right) = \frac{\text{K}_2\text{O}(\text{Diss.}) \cdot 2}{(2 \cdot 39.0983 + 15.9994)} \quad \text{Equation 4}$$

$Na^+ \left(\frac{\text{mol}}{\text{L}} \right)_{cem} = \frac{Na^+ \left(\frac{\text{mol}}{\text{g}} \right)}{w_{free}(L)}$ <p>(a)</p>	$Na^+ \left(\frac{\text{mol}}{\text{L}} \right)_{cm} = Na^+ \left(\frac{\text{mol}}{\text{g}} \right)_{cem} \cdot \frac{M_{cem}}{M_{cm}}$ <p>(b)</p>	Equation 5
$K^+ \left(\frac{\text{mol}}{\text{L}} \right)_{cem} = \frac{K^+ \left(\frac{\text{mol}}{\text{g}} \right)}{w_{free} \left(\frac{L}{g} \right)}$ <p>(a)</p>	$K^+ \left(\frac{\text{mol}}{\text{L}} \right)_{cm} = K^+ \left(\frac{\text{mol}}{\text{L}} \right)_{cem} \cdot \frac{M_{cem}}{M_{cm}}$ <p>(b)</p>	Equation 6
$w_{free} \left(\frac{L}{g} \right) = \frac{\frac{w}{cm} - 0.23\alpha_{cm}}{1000}$ <p>(a)</p>	$w_{free} \left(\frac{L}{g} \right) = \frac{\frac{w}{cm} - 0.23\alpha_{cm} \cdot \frac{M_{cem}}{M_{cm}}}{1000}$ <p>(b)</p>	Equation 7

Where:

- $Na_2O(Diss.)$ and $K_2O(Diss.)$ are the fractions of cementitious mass (%/100) which dissolve into the solution in the form of sodium oxide and potassium oxide
- cem is the cement portion, cm is the total cementitious
- $m_{f,i}^{(Na_2O)}$ and $m_{f,i}^{(K_2O)}$ are the mass fractions of the sodium oxide and potassium oxide in the cementitious material “i” (%/100)
- f_i is the free alkali ion factor of the cementitious material “i” (%/100)
- M_i is the mass fraction of a certain cementitious material
- $\frac{M_{cem}}{M_{cm}}$ is the mass fraction of cement with respect to the total cementitious materials mass (%/100)
- 22.9898 is the molar mass of sodium (g/mol)
- 39.0983 is the molar mass of potassium (g/mol)
- 15.9994 is the molar mass of potassium (g/mol)
- $w_{free} \left(\frac{L}{g} \right)$ is the mass of free water, which is the sum of the evaporable water present in the capillary and gel pores of the cementitious matrix, is estimated as described in Equation 8.
- DOR is the degree of hydration or reaction of the cementitious materials
- w/cm is the water to cementitious ratio

By combining Equation 1 and Equation 7:

$$Na^+ \left(\frac{\text{mol}}{\text{L}} \right) = \frac{\sum_i^n \left(2m_{f,i}^{(Na_2O)} \cdot \frac{M_i}{M_{cm}} \cdot f_i \cdot 0.75 \right)}{(2 \cdot 22.9898 + 15.9994)} \cdot \frac{1000}{\frac{w}{cm} - 0.23 \cdot DOR \cdot \frac{M_{cem}}{M_{cm}}}$$

Equation 8

$$K^+ \left(\frac{\text{mol}}{\text{L}} \right) = \frac{\sum_i^n \left(2m_{f,i}^{(K_2O)} \cdot \frac{M_i}{M_{cm}} \cdot f_i \cdot 0.75 \right)}{(2 \cdot 39.0983 + 15.9994)} \cdot \frac{1000}{\frac{w}{cm} - 0.23 \cdot DOR \cdot \frac{M_{cem}}{M_{cm}}} \quad \text{Equation 9}$$

$$f_{Na^+, Fly Ash} = \frac{\Delta IC_{(Na^+)} \cdot \left(\frac{w}{cm} - 0.23 \cdot DOR \right)}{1000 \cdot \frac{2m_f^{(Na_2O)} \cdot \frac{M_i}{M_{cm}}}{(2 \cdot 22.9898 + 15.9994)}} \quad \text{Equation 10}$$

$$f_{K^+, Fly Ash} = \frac{\Delta IC_{(K^+)} \cdot \left(\frac{w}{cm} - 0.23 \cdot DOR \right)}{1000 \cdot \frac{2m_f^{(K_2O)} \cdot \frac{M_i}{M_{cm}}}{(2 \cdot 22.9898 + 15.9994)}} \quad \text{Equation 11}$$

The estimated ionic concentrations are then used in an electrochemical model, developed by Snyder et al. [1], to calculate the pore solution electrical resistivity of the solution. Equation 12 uses the concentrations of the primary ionic species found in the pore solution (Na^+ , K^+ , OH^-) to estimate the pore solution resistivity [1].

This electrochemical model was found to be accurate within 8 % of the predicted resistivity for ionic strengths as high as 2 M and for potassium to sodium molar ratios from 1:1 to 4:1 in synthetic solutions [1].

$$\rho_{calc} = \frac{1}{\sum_i z_i c_i \lambda_i} \quad \text{Equation 12}$$

Where:

- ρ_{calc} is the calculate electrical resistivity of the pore solution (Ohm-m)
- z_i is the oxidation number (~) of the ionic species 'i'
- c_i , is the molar concentration (mol/L) of the ionic species 'i'
- λ_i is the equivalent conductivity (cm^2 S/mol) of the ionic species 'i'

Reference

- [1] K. . Snyder, X. Feng, B. . Keen, and T. . Mason, "Estimating the electrical conductivity of cement paste pore solutions from OH^- , K^+ and Na^+ concentrations," *Cem. Concr. Res.*, vol. 33, no. 6, pp. 793–798, Jun. 2003, doi: 10.1016/S0008-8846(02)01068-2.